*J Physiol* 589.21 (2011) pp 5193–5211



The Journal of Physiology

# Rearrangement of energetic and substrate utilization networks compensate for chronic myocardial creatine kinase deficiency

Petras P. Dzeja[1], Kirsten Hoyer[2], Rong Tian[2], Song Zhang[1], Emirhan Nemutlu[1], Matthias Spindler[2] and Joanne S. Ingwall[2]

[1]*Division of Cardiovascular Diseases, Departments of Internal Medicine and Molecular Pharmacology and Experimental Therapeutics, Mayo Clinic, Rochester, MN, USA*
[2]*Division of Cardiovascular Medicine, Department of Medicine, Brigham and Women's Hospital and Harvard Medical School, Boston, MA, USA*

**Non-technical summary** Continuous and vigorous heart work is powered by the energetic grid consisting of mitochondria, miniature ATP-generating fuel cells, and molecular connecting circuits transferring and distributing high-energy phosphoryls. The creatine kinase (CK) phosphotransfer circuit is the major component of the energetic network, coupling mitochondria with ATP utilization sites, and CK deficiency is a hallmark of cardiovascular diseases. Identification of mechanisms that compensate for reduced CK function would foster approaches leading to recovery and repair of injured hearts. Here, using advanced stable isotope metabolic technologies, we demonstrate that genetic CK deficiency induces a shift in heart energy distribution and substrate utilization networks by redirecting phosphotransfer flux through alternative adenylate kinase, glycolytic and guanine nucleotide systems. Such energetic re-wiring, together with increased mitochondrial and glycolytic capacities, defines an adaptive metabolomic phenotype of CK deficiency. These findings advance our understanding of cellular energetic infrastructure and provide new perspectives for regulation of energy distribution in disease states.

**Abstract** Plasticity of the cellular bioenergetic system is fundamental to every organ function, stress adaptation and disease tolerance. Here, remodelling of phosphotransfer and substrate utilization networks in response to chronic creatine kinase (CK) deficiency, a hallmark of cardiovascular disease, has been revealed in transgenic mouse models lacking either cytosolic M-CK (M-CK$^{-/-}$) or both M-CK and sarcomeric mitochondrial CK (M-CK/ScCKmit$^{-/-}$) isoforms. The dynamic metabolomic signatures of these adaptations have also been defined. Tracking perturbations in metabolic dynamics with $^{18}$O and $^{13}$C isotopes and $^{31}$P NMR and mass spectrometry demonstrate that hearts lacking M-CK have lower phosphocreatine (PCr) turnover but increased glucose-6-phosphate (G-6-P) turnover, glucose utilization and inorganic phosphate compartmentation with normal ATP $\gamma$-phosphoryl dynamics. Hearts lacking both M-CK and sarcomeric mitochondrial CK have diminished PCr turnover, total phosphotransfer capacity and intracellular energetic communication but increased dynamics of $\beta$-phosphoryls of ADP/ATP, G-6-P and $\gamma$-/$\beta$-phosphoryls of GTP, indicating redistribution of flux through adenylate kinase (AK), glycolytic and guanine nucleotide phosphotransfer circuits. Higher glycolytic and mitochondrial capacities and increased glucose tolerance contributed to metabolic resilience of M-CK/ScCKmit$^{-/-}$ mice. Multivariate analysis revealed unique metabolomic signatures for M-CK$^{-/-}$ and M-CK/ScCKmit$^{-/-}$ hearts suggesting that rearrangements in phosphotransfer and substrate utilization networks provide compensation for genetic CK deficiency. This new information highlights the significance of integrated CK-, AK-, guanine nucleotide- and glycolytic



DOI: 10.1113/jphysiol.2011.212829

enzyme-catalysed phosphotransfer networks in supporting the adaptivity and robustness of the cellular energetic system.

(Received 23 June 2011; accepted after revision 27 August 2011; first published online 30 August 2011)
**Corresponding authors** P. Dzeja: Mayo Clinic, 200 First Street SW, Stabile 5, Rochester, MN 55905, USA. Email: dzeja.petras@mayo.edu; Joanne Ingwall: Brigham and Women's Hospital, HIM-827, 221 Longwood Ave, Boston, MA 02115, USA. Email: jingwall@rics.bwh.harvard.edu

**Abbreviations** AK, adenylate kinase; BB-CK, brain-type creatine kinase; CK, creatine kinase; 2-DG, 2-deoxyglucose; 2-DG-6-P, 2-deoxyglucose-6-phosphate; GC-MS, gas chromatography-mass spectroscopy; $\Delta G_{ATP}$, free energy of ATP hydrolysis; G-6-P, glucose-6-phosphate; IPGTT, intraperitoneal glucose tolerance test; ITT, insulin tolerance test; M-CK, cytosolic M isoform of creatine kinase; NDPK, nucleoside diphosphate kinase; NMPK, nucleoside monophosphate kinase; OGTT, oral glucose tolerance test; PCA, principal component analysis; PCr, phosphocreatine; PLS-DA, partial least squares discriminant analysis; ScCKmit, sarcomeric mitochondrial creatine kinase isoform; VIP, variable importance in the projection.

## Introduction

Maintaining a robust bioenergetic and metabolic infrastructure is critical for preserving cell phenotype and survival under stress (Katz *et al.* 2003; Dzeja *et al.* 2007*a*; Feala *et al.* 2009; Jones & Thompson, 2009; Kuiper *et al.* 2009; Chung *et al.* 2010; Gohil *et al.* 2010; Jeninga *et al.* 2010; Hardie, 2011). Creatine kinase (CK)-catalysed phosphotransfer is the major component of the high-energy phosphoryl transfer and distribution network coupling ATP production in mitochondria with ATP utilization sites in excitable tissues (Ingwall *et al.* 1985; Wallimann *et al.* 1992; Saks *et al.* 1994). CK also plays an important role in energy supply required for cell division, cell motility and ion homeostasis in other cell types (Wyss *et al.* 2007; Kuiper *et al.* 2009) and can have a structural role independent of catalytic activity by stabilizing plasma membrane $Na^+$–$Ca^{2+}$ exchanger activity (Yang *et al.* 2010). Importantly, compromised CK function is a hallmark of abnormal bioenergetics in cardiovascular, neural and other human diseases (Ingwall *et al.* 1985; Neubauer *et al.* 1997; Cha *et al.* 2003; Dahlstedt *et al.* 2003; Saks *et al.* 2006; Wyss *et al.* 2007; Bottomley *et al.* 2009; Ventura-Clapier *et al.* 2010). Reduced CK flux is the most prominent metabolic abnormality observed in human heart failure and myocardial infarction (Bottomley *et al.* 2009). Identifying mechanisms that compensate for reduced CK function would advance our understanding of cellular energetic systems and facilitate development of approaches leading to recovery and repair of injured hearts (Taegtmeyer *et al.* 1997; Dzeja *et al.* 1999; Pucar *et al.* 2001; Tian, 2003; Cha *et al.* 2006; Ingwall, 2009; Kolwicz & Tian, 2009). However, the adaptive phosphotransfer pathways and rearrangements in the bioenergetic system in CK-deficient hearts are poorly understood.

Studies of transgenic animal models have revealed an inherent plasticity of the cellular energetic network and the development of cytoarchitectural and metabolic compensatory mechanisms in striated muscles (van Deursen *et al.* 1993; Dzeja *et al.* 1998, 2004; Janssen *et al.* 2000, 2003; Pucar *et al.* 2000; de Groof *et al.* 2001; Bruton *et al.* 2003; Ingwall, 2004, 2006; Ventura-Clapier *et al.* 2004). However, hearts deficient in the major CK isoforms under increased functional load cannot sustain normal global ATP/ADP ratios, indicating compromised communication between ATP-consuming and ATP-generating cellular sites (Nicolay *et al.* 1998; Saupe *et al.* 1998, 2000; Katz *et al.* 2003; Ingwall, 2004). This renders contractions to be more energetically costly, forcing the heart to operate under less efficient energetics under stress (Saupe *et al.* 1998, 2000). Such energetic abnormalities reduce the ability of the myocardium to respond to $\beta$-adrenergic stimulation (Crozatier *et al.* 2002), and CK-deficient hearts are more vulnerable to ischaemia-reperfusion injury (Spindler *et al.* 2004). In addition, CK-deficient hearts, despite cytoarchitectural adaptations (Ventura-Clapier *et al.* 1995; Boehm *et al.* 2000), cannot sustain adequate subsarcolemmal nucleotide exchange and have increased electrical instability under metabolic stress (Abraham *et al.* 2002).

Among alternative phosphotransfer pathways, the adenylate kinase (AK)-catalysed circuit is a likely candidate that can provide compensation in CK-deficient hearts (Dzeja *et al.* 1999, 2002, 2007*b*; Dzeja & Terzic, 2003). Studies of AK1 and AK2 gene deficiencies have shown that AK-catalysed phosphoryl transfer contributes to metabolic efficiency, maintenance of adenine nucleotide pool size, mitochondrial ATP export, inter-organellar energetic communication and execution of developmental programming (Pucar *et al.* 2000, 2002; Dzeja *et al.* 2002, 2007*a*; Noma, 2005; Lagresle-Peyrou *et al.* 2009; Pannicke *et al.* 2009). Moreover, it is known that metabolic flux through the AK system increases in failing hearts and during oxygen deprivation (Dzeja *et al.* 1999; Pucar *et al.* 2004), as well as in muscles with chemically or genetically inhibited activity of CK (Dzeja *et al.* 1996, 2004). The network of glycolytic/glycogenolytic reactions can also provide high-energy phosphoryl transferring capacity between cellular compartments (Dzeja & Terzic,

2003; Dzeja *et al.* 2004; Chung *et al.* 2010), and glycolytic enzymes are upregulated in muscles of CK-deficient mice and in failing hearts (Ventura-Clapier *et al.* 1995; Boehm *et al.* 2000; de Groof *et al.* 2001; Katz *et al.* 2003; Dzeja *et al.* 2004; Aksentijevic *et al.* 2010). In addition, enzymes involved in guanine nucleotide phosphotransfer, such as nucleoside diphosphate kinase (NDPK) and guanylate kinase, have specific energetic and signal transduction regulatory roles (Janssen *et al.* 2000; Dzeja & Terzic, 2003; Dzeja *et al.* 2007*a*; Hippe *et al.* 2009). Yet, changes in metabolic fluxes through AK, glycolytic and guanine nucleotide phosphotransfer circuits and substrate utilization in hearts lacking either M-CK or both M-CK and the mitochondrial isoform ScCKmit have not been determined.

To define rearrangements in metabolic networks and compensatory mechanisms for CK deficiency, the dynamics of high-energy phosphoryl exchange among CK, AK, glycolytic and guanylate systems and substrate utilization were followed in wild type and transgenic mouse hearts lacking either cytosolic M-CK (M-CK$^{-/-}$) or both M-CK and mitochondrial CK (M-CK/ScCKmit$^{-/-}$). This was done using advanced phosphoryl $^{18}$O-labelling analysis with gas chromatography-mass spectroscopy (GC-MS) and substrate uptake and metabolism with $^{13}$C and $^{31}$P NMR techniques and metabolomic analysis software. We demonstrate that lack of one or both major CK isoforms induces specific dynamic rearrangements in the cellular bioenergetic infrastructure defined by increased mitochondrial and glycolytic capacities and metabolic load on the remaining CK isozymes, AK, glycolytic and guanine nucleotide phosphotransfer systems along with a shift in substrate utilization, all contributing to distinct energetic and metabolomic phenotypes.

## Methods

### Animal description and ethical approval

Adult wild type mice (strain C57/BL6) and transgenic mice lacking either the genes for the cytosolic CK isoform (M-CK$^{-/-}$) or both M-CK and the sarcomeric mitochondrial CK isoforms (M-CK/ScCKmit$^{-/-}$) were used. Details on the genetic background and generation of mutant animals have been reported (van Deursen *et al.* 1993; Steeghs *et al.* 1997). The investigation conformed to the *Guidelines for the Care and Use of Laboratory Animals* of the National Institutes of Health, and was approved by the Institutional Animal Care and Use Committee at the University of Minnesota, the Mayo Clinic and Harvard University. The authors have read, and the experiments comply with, the policies and regulations of *The Journal of Physiology* given by Drummond (2009).

### Isolated heart perfusion with $^{18}$O-enriched media

Hearts were excised and perfused in the Langendorff mode as described in detail previously (Saupe *et al.* 1998, 2000). After 30 min, the perfusate was switched to a media enriched with 20% [$^{18}$O]$H_2O$ (Isotec Inc.). Hearts were perfused for 20, 40 or 60 s and then freeze-clamped in liquid $N_2$ and stored in liquid $N_2$ until analysis. At the 60 s time point labelling showed an apparent saturation, therefore all subsequent measurements were done at 20 and 40 s time points.

### Purification and isotopic analysis of $^{18}$O-labelled cellular phosphoryls using HPLC and GC-MS

Freeze-clamped hearts were pulverized in a mortar with liquid nitrogen, and extracted in a solution containing 0.6 M $HClO_4$ and 1 mM EDTA (Zeleznikar *et al.* 1995; Dzeja *et al.* 1996, 1999). Cellular ATP, ADP, GTP, GDP, inorganic phosphate, creatine phosphate (CrP) and glucose-6-phosphate (G-6-P) were purified and quantified using HPLC. The $\gamma$-phosphoryls of ATP or GTP were transferred to glycerol by glycerokinase, while $\beta$-phosphoryls of ATP and ADP were transferred to glycerol by a combined action of AK and glycerokinase. The $\beta$-phosphoryls of GTP and GDP were transferred to glycerol by a combined catalytic action of guanylate kinase (GK) and glycerokinase (Dzeja *et al.* 1996; Janssen *et al.* 2000). The phosphoryl of CrP was transferred to $\gamma$-ATP by CK, and then to glycerol using glycerokinase (Dzeja *et al.* 1996). Samples containing phosphoryls of $\gamma$-ATP, $\beta$-ATP, $\beta$-ADP, $\gamma$-GTP, $\beta$-GTP, $\beta$-GDP, CrP, as glycerol 3-phosphate, and inorganic phosphate were converted to their respective trimethylsilyl derivatives. The $^{18}$O enrichment of phosphoryls in glycerol 3-phosphates was determined with a Hewlett-Packard 5970B gas chromatograph-mass spectrometer operated in the select ion-monitoring mode. The percentage of nucleotide phosphoryl oxygens replaced by $^{18}$O was calculated according to the formula: [% $^{18}O_1 + 2$(% $^{18}O_2$) + 3(% $^{18}O_3$)]/3(% $^{18}$O in $H_2O$) (Dzeja *et al.* 1996, 1999).

### Analysis of $^{18}$O labelling data and cellular phosphotransfer dynamics

ATP turnover and phosphoryl flux through the AK, CK, glycolytic and guanylate systems were measured in perfused hearts using the $^{18}$O-phosphoryl labelling technique (Zeleznikar *et al.* 1990, 1995; Dzeja *et al.* 1996, 1999). The $^{18}$O labelling procedure is based on incorporation of one $^{18}$O atom, provided from [$^{18}$O]$H_2O$, into inorganic phosphate with each act of ATP hydrolysis and the subsequent distribution

**Table 1. Reactions and heart energetic parameters measured**

| Reaction | Parameters |
|---|---|
| $\gamma$ATP + [$^{18}$O] $H_2O$ → [$^{18}$O] $P_i$ + ADP | ATP hydrolysis |
| [$^{18}$O] $P_i$ + ADP → [$^{18}$O] $\gamma$ATP | ATP synthesis |
| [$^{18}$O] $\gamma$ATP + Cr → [$^{18}$O] CrP + ADP | CK-catalysed phosphotransfer |
| [$^{18}$O]$\gamma$ATP+AMP→[$^{18}$O]$\beta$ADP + ADP→[$^{18}$O]$\beta$ATP + AMP | AK-catalysed phosphotransfer |
| [$^{18}$O]$\gamma$ATP+glucose → [$^{18}$O]glucose-6-P + ADP | Hexokinase-catalysed phosphotransfer |
| [$^{18}$O]$\gamma$ATP + GMP → [$^{18}$O]$\beta$GDP + ADP | GK-catalysed phosphotransfer |
| [$^{18}$O]$\gamma$ATP+GDP → [$^{18}$O]$\gamma$GTP + ADP | NDPK/succinyl-CoA synthase phosphotransfer |
| [$^{18}$O] $P_i$/[$^{18}$O]$\gamma$ATP ratio | Energetic communication between ATP utilization and synthesis sites |

of $^{18}$O-labelled phosphoryls among other high-energy phosphoryl-carrying molecules (Dawis *et al.* 1989; Zeleznikar & Goldberg, 1991). This permits monitoring of energetic dynamics with determination of ATP consumption and synthesis rates, high-energy phosphoryl transfer by creatine kinase, adenylate kinase and glycolytic reactions, and energetic communication between intracellular ATP hydrolysis and ATP synthesis sites (Pucar *et al.* 2001; Dzeja *et al.* 2007*b*). Monitoring kinetics of isotopic labelling provides a means of quantifying metabolite turnover rates and fluxes through individual enzymatic pathways using classical approaches (Zilversmit *et al.* 1943; Rossi, 1975; Karl & Bossard, 1985; Dawis *et al.* 1989; Olson *et al.* 1996), and computer modelling of labelling kinetics and label distribution throughout metabolic networks (Zeleznikar *et al.* 1990; Wiechert & de Graaf, 1997; Metallo *et al.* 2009). The reactions and heart energetic parameters measured are given in Table 1.

The cellular ATP turnover rate was estimated from the sum of the total number of $^{18}$O atoms appearing in phosphoryl-containing metabolites and orthophosphate after each act of ATP hydrolysis (Zeleznikar *et al.* 1990). The net rate of AK-catalysed phosphotransfer was determined from the rate of appearance of $^{18}$O-containing $\beta$-phosphoryls in ADP and ATP as described previously (Dawis *et al.* 1989; Zeleznikar *et al.* 1990, 1995; Olson *et al.* 1996). AK-mediated $\beta$-phosphoryl labelling rate was calculated as ((($^{18}$O labelling (%) of $\beta$-ADP/100)$*$[$\beta$-ADP]$*$3) + ($^{18}$O labelling (%) of $\beta$-ATP/100)$*$[$\beta$ATP]$*$3)/$t$), where [$\beta$-ADP] and [$\beta$-ATP] are nucleotide concentrations and $t$ is the labelling time (Zeleznikar *et al.* 1990, 1995; Olson *et al.* 1996). To estimate AK phosphotransfer flux, kinetics and total number of $^{18}$O-labelled phosphoryls in $\beta$-ADP and $\beta$-ATP produced by the AK catalysis, precursor $\gamma$-ATP labelling kinetics, kinetics of label loss from a metabolite pool as well as metabolically active metabolite pool size are considered (Dawis *et al.* 1989; Zeleznikar *et al.* 1990, 1995). Such kinetic analysis permits establishing the relationship between measured metabolite labelling rate and metabolic flux through a specific pathway (Zeleznikar *et al.* 1990). Knowing the kinetic relationship, AK metabolic flux can be deduced from the labelling data at the specific time point in the initial pseudo-linear labelling curve. The AK flux represents the amount of ADP that would have to be metabolized by AK to form AMP and produce the observed magnitude of $^{18}$O-labelled $\beta$-ADP and $\beta$-ATP within the times examined.

The net rate of CK-catalysed phosphoryl transfer was determined from the rate of appearance of $^{18}$O-labelled phosphoryls in PCr (Zeleznikar *et al.* 1990; Dzeja *et al.* 1996). The cumulative percentage of phosphoryl oxygens replaced by $^{18}$O in $\gamma$-ATP and CrP was calculated as [% $^{18}O_1 + 2(\%\ ^{18}O_2) + 3(\%\ ^{18}O_3)$]/[3(% $^{18}$O in $H_2O$)] (Dzeja *et al.* 1996; Olson *et al.* 1996). The number of CrP labelled phosphoryls is calculated as (% $^{18}O_1$ + 2(% $^{18}O_2$) +3 (% $^{18}O_3$)/(0.488$*$100))$*$100, where 0.488 is a theoretical $^{18}$O incorporation at 20% $H_2$[$^{18}$O]. The CK-mediated CrP labelling rate is calculated as (($^{18}$O labelling (%) of CrP/100)$*$[CrP]$*$3)/$t$, where [CrP] is concentration, $t$ is the labelling time; a factor of 3 is used since there are three possible bonds for $^{18}$O incorporation in phosphoryl of CrP. Since CrP labelling rate is high and close to that of $\gamma$-ATP, the precursor labelling rate, a gradual inhibition of CK is necessary to calculate CrP turnover rate and for establishing the relationship between measured CrP $^{18}$O-labelling kinetics and predicted CK metabolic flux (Zeleznikar *et al.* 1995; Dzeja *et al.* 1996). After determining such a relationship, CK metabolic flux can be deduced from the labelling data at a specific time point in the initial pseudo-linear labelling curve as ($^{18}$O labelling (%) of CrP/100)$*$[CrP]$*3*\rho$, where $\rho$ is the slope of the correlation curve. The rates of phosphoryl flux through the glycolytic and guanine nucleotide phosphotransfer systems were quantified in a similar way from the appearance of $^{18}$O-labelled phosphoryls in G-6-P and in $\gamma$- and $\beta$-GTP/GDP (Dzeja *et al.* 1999; Janssen *et al.* 2000; Pucar *et al.* 2000).

### Measurements of basal and insulin-stimulated glucose uptake and substrate utilization using $^{13}C$ and $^{31}P$ NMR

The rate of glucose uptake was measured in isolated perfused hearts by $^{31}P$ NMR using the glucose analogue 2-deoxyglucose (2-DG) (5 mM glucose was replaced with 5 mM 2-DG in the Krebs–Henseleit buffer) (Hopkins *et al.* 2004). Ten consecutive 8 min $^{31}P$ NMR spectra of intracellular 2-deoxyglucose-6-phosphate (2-DG-6-P) were obtained. Insulin (2 mU ml$^{-1}$) was then added to the perfusate and another four $^{31}P$ NMR spectra were collected to assess the maximal rate of insulin-stimulated glucose transport. In another group of isolated mouse hearts, hearts were perfused with Krebs–Henseleit buffer containing a mix of long-chain fatty acids bound to 1% albumin (palmitic acid, palmitoleic acid, oleic acid and linoleic acid), DL-$\beta$-hydroxybutyrate, lactate and 50 mU ml$^{-1}$ insulin. Hearts were perfused with all substrates, among which two were $^{13}C$ enriched. In one series, [U-$^{13}C$] fatty acid and [3-$^{13}C$] lactate were supplied to determine the relative contributions of fatty acid and lactate to acetyl-CoA production. Identical experiments with enriched [U-$^{13}C$] glucose and [2,4-$^{13}C$] $\beta$-hydroxybutyrate determined the relative contributions of these two substrates to oxidative metabolism. $^{13}C$ NMR spectra of cardiac tissue extract were acquired using a 3 mm NMR probe (Varian Medical Systems) (Luptak *et al.* 2007). The contributions of each labelled substrate to the oxidative metabolism were determined using the $^{13}C$ isotopomers peak areas of the C3 and C4 of glutamate by modelling the tricarboxylic acid cycle flux (Malloy *et al.* 1988, 1990).

### Enzyme activities and metabolite levels

CK activity in extracts from frozen powdered tissue was determined spectrophotometrically (Dzeja *et al.* 1999). Electrophoretic separation and quantification of CK isoforms in myocardial extracts were done using the Hydragel ISO-CK K20 kit (Sebia). Zymogram scans were analysed with the FluorChem Imaging System and AlphaEaseFC software (Cell Biosciences). Protein content was determined by the BCA method (Pierce Chemical Co.). Myocardial ATP, ADP, AMP, CrP and G-6-P levels were determined in perchloric acid extracts using HPLC and coupled enzyme assays (Dzeja *et al.* 1996, 1999). Muscle inorganic phosphate level was determined in perchloric acid extracts using the EnzChek Phosphate Assay kit (Molecular Probes).

### Glycolytic and mitochondrial capacities

Glycolytic capacity was determined from the maximal rate of glucose conversion to lactate in heart muscle homogenates (Phillips *et al.* 2010). Mitochondrial oxidative capacity was assessed by measuring citrate synthase activity using the Citrate Synthase Assay Kit (Sigma).

### Glucose and insulin tolerance tests

For the intraperitoneal glucose tolerance test (IPGTT), after 6 h of fasting glucose load was administered to wild type and M-CK/ScCKmit$^{-/-}$ mice by intraperitoneal injection of D-glucose (2 g kg$^{-1}$). Blood samples were taken from the tail vein before and after the glucose load. For the oral glucose tolerance test (OGTT), a bolus of glucose (2 g kg$^{-1}$) was delivered into the stomach by a gavage needle and blood was sampled for plasma glucose and insulin analyses. Blood glucose was measured using a Lifescan One Touch Basic Glucometer kit (Johnson & Johnson). For the insulin tolerance test (ITT), after 3 h of fasting insulin (Novo Nodisk) was administered to wild type and M-CK/ScCKmit$^{-/-}$ mice by intraperitoneal injection (0.5 U (kg body weight)$^{-1}$). Blood samples were taken before and after the insulin load. Blood was immediately centrifuged, and the plasma was separated and stored at –20°C until assayed. Plasma insulin levels were assayed using the Insulin (Mouse) Ultrasensitive EIA kit (Alpco Diagnostics).

### Data analysis for dynamic metabolomic profiling

Principal component analysis (PCA) and partial least-squares discriminant analysis (PLS-DA) was utilised as modelling methods for clustering and discrimination (Rayens & Andersen, 2006). PCA score plots are used to investigate any outlier in the sample and also run to detect any inherent trends within the data. As seen in Supplementary Fig. 2S*A*, there is not any outlier or inherent trends in the data and there is very clear separation between groups. Examination of the corresponding loading plot indicated those metabolites responsible for the clustering of groups (Fig. 2S*B*). Metabolites located centre of the plot do not contribute to the clustering of the animal groups, whereas those in the same geographical region of a sample group in the corresponding score plot are responsible for the separation (for example, G-6-P and lactate utilization are higher in the M-CK$^{-/-}$ group). Validation of the PLS-DA model was done by comparison with the classification statistics of models generated after (20) random permutations of the class matrix. The model $R^2$ and $Q^2$ values on the right were higher than those obtained in random permuted models across all 20 iterations (Fig. 2S*C*). $R^2$ relates to the explained variance, i.e. the ability to describe data, whereas $Q^2$ summarizes the predictive variance, i.e. the ability to predict correctly new data. The value of $Q^2$ ranges from 0 to 1 and typically a $Q^2$ value of greater than 0.4 is considered

as a good model, and those with $Q^2$ values over 0.7 are robust (Titman *et al.* 2009). In our case, the $Q^2$ and $R^2$ were higher than 0.88 in both discrimination. All of these results indicate that the methods are a good model and robust. PLS-DA is a pattern-recognition technique that correlates variation in the data set with class membership. The VIP (variable importance in the projection) values (Le Moyec *et al.* 2005), a weighted sum of squares of the PLS weight, which indicates the importance of the variable to the whole model, were calculated to identify the most important molecular variables for the clustering of specific groups. Calculation of the PLS-DA model parameters was carried out using SIMCA-P+ (v12.0, Umetrics AB, Umea, Sweden).

### Statistical analysis

All data are expressed as mean ± SEM. Student's unpaired *t* test was used and differences were considered statistically significant at $P < 0.05$. To test for differences among the groups one-way ANOVA was used.

## Results

### Enzyme activity and functional performance

Deletion of the genes encoding cytosolic M-CK and mitochondrial ScCKmit markedly reduced myocardial CK activity. Total CK catalytic capacity, measured using conventional coupled enzyme assay, for wild type, M-CK$^{-/-}$ and M-CK/ScCKmit$^{-/-}$ hearts was 7.98 ± 0.92, 2.27 ± 0.26 and 0.24 ± 0.02 $\mu$mol min$^{-1}$ (mg protein)$^{-1}$, respectively ($n = 6$ in each group). In the normal mouse heart the cytosolic MM-CK isoform contributes ∼60% to total CK activity, brain-type creatine kinase (BB-CK) about 3%, while ScCKmit provides the remaining 37% (Saupe *et al.* 2000). Maximal CK catalytic capacities of wild type and M-CK$^{-/-}$ hearts exceed total myocardial ATP turnover rate, 0.380 $\mu$mol min$^{-1}$ (mg protein)$^{-1}$, calculated from oxygen consumption (Saupe *et al.* 1998) by 21 and 6 times, respectively, indicating the presence of significant phosphotransfer reserve. Contractile performance of hearts was not significantly different among wild type, M-CK$^{-/-}$ and M-CK/ScCKmit$^{-/-}$ hearts, although there was a trend of lower performance in double-mutant hearts. Values for the product of heart rate and developed pressure, RPP, were 30.3 ± 1.6, 30.4 ± 3.0 and 24.1 ± 3.2 ($P = 0.08$) mmHg min$^{-1}$ ×10$^3$ in wild type, M-CK$^{-/-}$ and M-CK/ScCKmit$^{-/-}$ hearts, respectively.

### Dynamics of intracellular phosphotransfer networks

Kinetic behaviour of CK catalysis in wild type, M-CK$^{-/-}$ and M-CK/ScCKmit$^{-/-}$ hearts (Fig. 1*A*) was assessed by measuring the rate of appearance of $^{18}$O-labelled phosphoryls in PCr resulting from CK-catalysed transfer of $\gamma$[$^{18}$O]-phosphoryls of ATP to creatine. This technique permits quantification of net phosphoryl flux through CK since there is no net gain or loss of $^{18}$O atoms in a series of unidirectional exchange reactions (Dzeja *et al.* 1996). CK-catalysed phosphotransfer in M-CK$^{-/-}$ hearts, which eliminates about 71% of total CK activity, resulted in a modest 23% ($n = 6$, $P < 0.05$) reduction in the rate of appearance of [$^{18}$O]PCr (Fig. 1*A*). This suggests a higher phosphotransfer load carried out by the ScCKmit and BB-CK isoforms. Deletion of both ScCKmit and MM-CK isoforms, which eliminates 97% of the total CK activity, diminished CK-catalysed phosphoryl transfer capability by over 88% (Fig. 1*A*). The remaining 12% of CK-mediated phosphotransfer can be attributed to the BB-CK isoform. Thus, although severely compromised, CK-catalysed phosphotransfer was not completely abolished by deleting both MM-CK and ScCKmit isoforms.

Appearance of $^{18}$O-labelled phosphoryls in $\beta$-ADP, an indicator of AK-catalysed phosphotransfer, was increased only marginally in response to deletion of the M-CK, but significantly, by 85% ($n = 6$, $P < 0.001$), in hearts with deletions of both M-CK and ScCKmit (Fig. 1*B*). These results indicate that a moderate reduction in CK phosphotransfer rate of ∼23%, due to deletion of the cytosolic MM-CK isoform, does not provoke an increase in AK flux, while compensation provided by AK is required when CK phosphotransfer rate is decreased by 88% caused by deletion of both MM-CK and ScCKmit isoforms.

Appearance of $^{18}$O-labelled phosphoryls in $P_i$, an indicator of cellular ATPase velocity, was reduced both in M-CK$^{-/-}$ and M-CK/ScCKmit$^{-/-}$ hearts ($n = 6$, $P < 0.05$) (Fig. 1*C*). Kinetics of $^{18}$O labelling indicates that $^{18}$O incorporation into $P_i$ in both types of CK-deficient hearts approaches saturation faster compared to wild type hearts. At 40 s of perfusion time with $^{18}$O-containing media $^{18}$O labelling of $P_i$ was 52.9 ± 3.1%, 43.1 ± 2.5% ($P < 0.05$) and 35.2 ± 2.3% ($P < 0.05$) in wild type, M-CK$^{-/-}$ and M-CK/ScCKmit$^{-/-}$ hearts, respectively ($n = 6$ each). The same difference in $P_i$ labelling also remained at 60 s (not shown), indicating that it approaches saturation. This suggests a smaller size of the metabolically active $P_i$ pool and increased compartmentation of $P_i$ in both types of CK-deficient hearts.

The rate of appearance of $^{18}$O-labelled phosphoryls in $\gamma$-ATP, an indicator of overall ATP synthesis, was not compromised in either transgenic heart (Fig. 1*D*) but several observations are consistent with less efficient energetics. There was a trend towards increased $\gamma$-ATP labelling in M-CK/ScCKmit$^{-/-}$ hearts, which is consistent with less efficient energetics due to the absence of both CK isoforms. Moreover, the $P_i/\gamma$-ATP $^{18}$O-labelling ratio, an indicator of intracellular energetic communication

between ATP utilization and ATP synthesis sites (Dzeja *et al.* 2007*b*), was reduced from $0.91 \pm 0.02$ in wild type to $0.80 \pm 0.03$ ($P < 0.05$) and $0.55 \pm 0.05$ ($P < 0.001$, $n = 6$) in M-CK$^{-/-}$ and M-CK/ScCKmit$^{-/-}$ hearts, respectively (Fig. 1*E*). This indicates that phosphoryl exchange between the ATPase compartment where $P_i$ gets $^{18}O$ incorporated and the ATP synthesis compartment, presumably in mitochondria where $\gamma$-ATP gets $^{18}O$-labelled $P_i$, is compromised in the absence of CK.

## Total cellular ATP turnover in relationship to CK and AK phosphotransfer fluxes

Total ATP turnover rate, obtained by counting all $^{18}O$ atoms appearing in $P_i$ and major metabolite phosphoryls after each event of ATP hydrolysis, was not significantly different among wild type and CK-deficient hearts (Fig. 2). Total ATP turnover was equal to $539 \pm 25$, $505 \pm 27$ and $473 \pm 20$ ($P = 0.06$) nmol ATP min$^{-1}$ (mg protein)$^{-1}$ ($n = 6$ each) in wild type, M-CK$^{-/-}$ and M-CK/ScCKmit$^{-/-}$

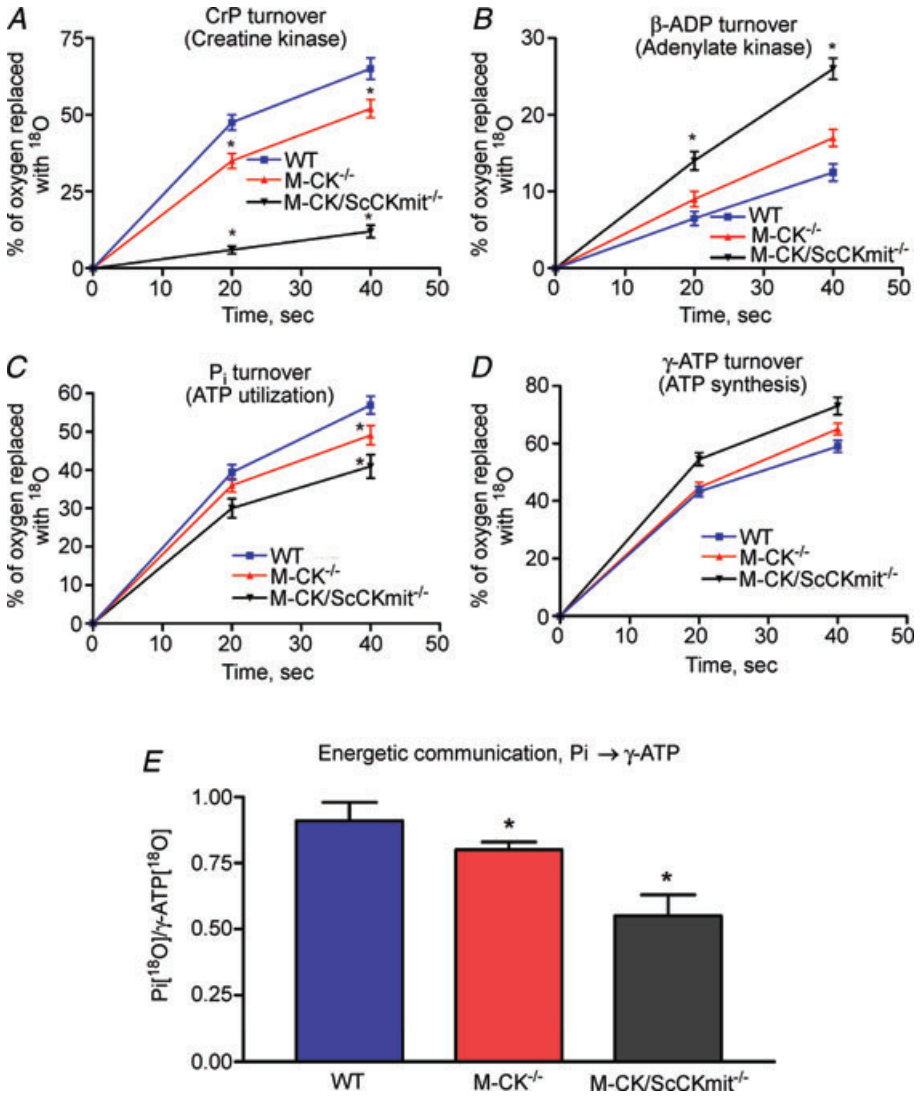


**Figure 1. Altered kinetics of high-energy phosphoryl exchange and energetic communication in hearts with CK gene deletions**
*A*, kinetics of $^{18}O$-labelled phosphoryl appearance in PCr representing CK metabolic flux in wild type (WT) *versus* M-CK$^{-/-}$ and M-CK/ScCKmit$^{-/-}$ hearts. *B*, kinetics of $^{18}O$-labelled phosphoryl appearance in $\beta$-phosphoryls of ATP indicating adenylate kinase metabolic flux. *C*, $^{18}O$-labelling of cellular inorganic phosphate (Pi) representing ATPase velocity and compartmentation of Pi. *D*, $^{18}O$-labelling of $\gamma$-phosphoryls of ATP indicating cellular ATP synthesis rate. *E*, changes in Pi/$\gamma$-ATP $^{18}O$-labelling ratio, an indicator of intracellular energetic communication between ATP utilization and synthesis sites. $n = 6$ in each group. $^*P < 0.05$.

hearts, respectively. Net phosphoryl flux through the CK-catalysed system was $368 \pm 26$, $282 \pm 18$ ($P < 0.05$) and $50 \pm 4$ ($P < 0.001$) nmol PCr $min^{-1}$ (mg protein)$^{-1}$ in wild type, M-CK$^{-/-}$ and M-CK/ScCKmit$^{-/-}$ hearts ($n = 6$ each), respectively. Net phosphoryl flux through the AK system (Fig. 2) was $96 \pm 9$, $112 \pm 11$ and $186 \pm 15$ ($P < 0.001$) nmol ADP $min^{-1}$ (mg protein)$^{-1}$ in wild type, M-CK$^{-/-}$ and M-CK/ScCKmit$^{-/-}$ hearts ($n = 6$ each), respectively. Thus, AK metabolic flux was nearly doubled in M-CK/ScCKmit$^{-/-}$ hearts, indicating a compensatory potential of this phosphotransfer system. Calculations show that correlation between AK flux and heart performance (RPP) was markedly increased in M-CK/ScCKmit$^{-/-}$ hearts. The correlation coefficient ($R$) was 0.34 in wild type, 0.49 in M-CK$^{-/-}$ and 0.83 ($P < 0.05$) in M-CK/ScCKmit$^{-/-}$ hearts, suggesting a greater dependence on energy delivered through the AK system in M-CK/ScCKmit$^{-/-}$ hearts. The sum of CK- and AK-mediated phosphoryl flux was equal to 86%, 78% and 50% of the total cellular ATP turnover in wild type, M-CK$^{-/-}$ and M-CK/ScCKmit$^{-/-}$ hearts, respectively. Thus, when compared to wild type, M-CK$^{-/-}$ hearts had normal ATP turnover rate with a minimal phosphotransfer deficit. In contrast, M-CK/ScCKmit$^{-/-}$ hearts maintained a near-normal ATP turnover rate despite a ~50% reduction in combined CK and AK phosphotransfer rate. This raises the possibility that additional compensatory mechanisms in metabolic networks contribute to the energetic homeostasis in CK-deficient hearts.

## Dynamics of high-energy phosphoryls in guanine and glycolytic phosphotransfer systems

We then examined two other cellular phosphotransfer pathways: glycolytic and guanine nucleotide phosphotransfer systems. Figure 3*A* and *B* shows $\gamma$- and $\beta$-phosphoryl turnover of GTP in WT, M-CK$^{-/-}$ and M-CK/ScCKmit$^{-/-}$ hearts. In WT hearts, GTP $\gamma$-phosphoryl turnover, as indicated from the appearance of $^{18}$O label (Fig. 3*A*), was robust and ~70% of $\gamma$-ATP turnover (Fig. 1*D*); at 20 and 40 s perfusion times, $\gamma$-GTP $^{18}$O labelling was $29.3 \pm 0.8$% and

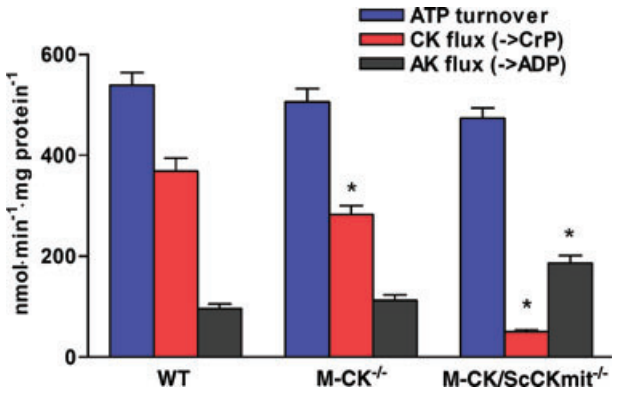


**Figure 2. Total cellular ATP turnover and interchange between CK and AK phosphotransfer fluxes**
Estimated rates of total ATP turnover, creatine kinase (CK) and adenylate kinase (AK) phosphoryl fluxes in wild type (WT), M-CK$^{-/-}$ and M-CK/ScCKmit$^{-/-}$ hearts. $n = 6$ in each group. *$P < 0.05$.

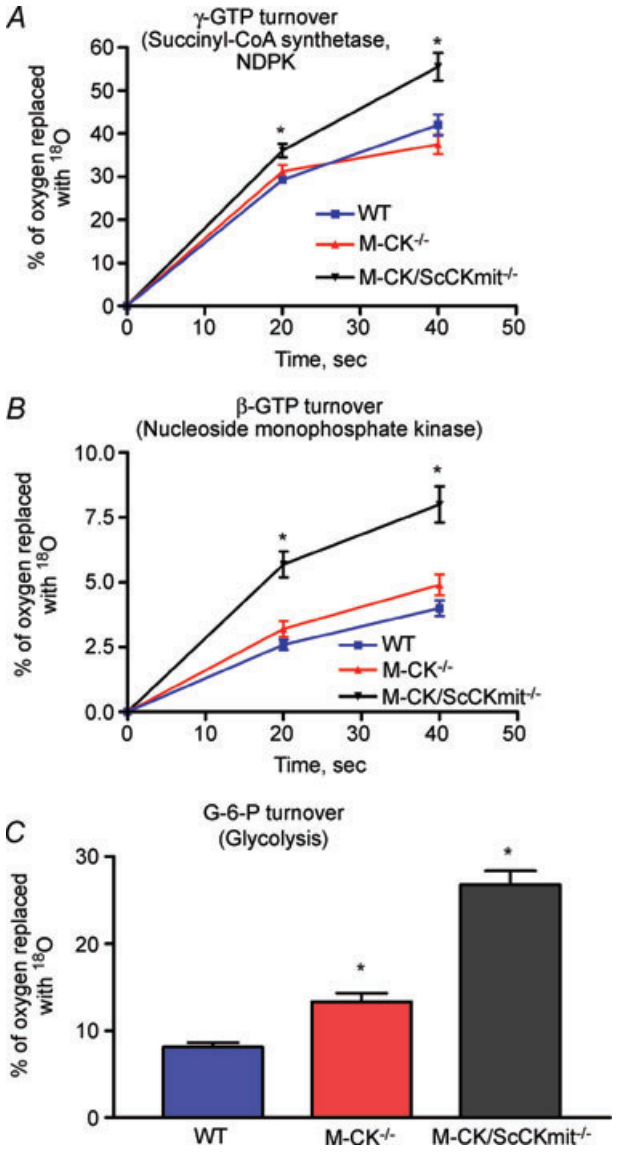


**Figure 3. Phosphotransfer redistribution through guanylate and glycolytic pathways and adjustment of overall energetic dynamics in CK-deficient hearts**
*A*, kinetics of $^{18}$O-labelled phosphoryl appearance in $\gamma$-GTP representing GTP synthesis rate in succinyl-CoA synthase (Krebs cycle) and nucleoside diphosphate kinase (NDPK) reactions in wild type (WT), M-CK$^{-/-}$ and M-CK/ScCKmit$^{-/-}$ hearts. *B*, kinetics of $^{18}$O-labelled phosphoryl appearance in $\beta$-phosphoryls of GTP representing metabolic flux through nucleoside monophosphate kinase (NMPK)-catalysed reactions. *C*, $^{18}$O-labelling of G-6-P signifying changes in glycolytic phosphotransfer rate.

42.0 ± 2.4%, respectively ($n = 6$). In M-CK$^{-/-}$ hearts, GTP $\gamma$-phosphoryl turnover was similar to WT hearts: 31.2 ± 1.5% and 37.5 ± 2.2% at 20 and 40 s, respectively ($n = 6$). However, in M-CK/ScCKmit$^{-/-}$ hearts GTP $\gamma$-phosphoryl turnover was significantly increased. GTP $^{18}$O labelling in M-CK/ScCKmit$^{-/-}$ hearts was 36.1 ± 0.9% and 55.5 ± 3.2% at 20 and 40 s, respectively ($P < 0.05$, $n = 6$), representing a 23% and 32% increase over WT values. Therefore, $\gamma$-GTP turnover, reflecting metabolic flux through the Krebs cycle enzyme succinyl CoA synthase and NDPK, was augmented only with severe CK deficiency in M-CK/ScCKmit$^{-/-}$ hearts.

Turnover of $\beta$-phosphoryl of GTP, an indicator of nucleoside monophosphate kinase (NMPK)-catalysed phosphotransfer, was unaltered in M-CK$^{-/-}$ hearts, but was substantially increased in M-CK/ScCKmit$^{-/-}$ hearts compared to WT hearts (Fig. 3*B*). At 20 and 40 s of labelling, $\beta$-GTP $^{18}$O labelling was 2.6 ± 0.2% and 4.0 ± 0.3% in WT, 3.2 ± 0.3% and 4.5 ± 0.4% in M-CK$^{-/-}$ and 5.7 ± 0.5% and 8.0 ± 1.2% in M-CK/ScCKmit$^{-/-}$ hearts ($n = 6$ each), respectively. Thus, the turnover of $\beta$-phosphoryls of GTP in M-CK/ScCKmit$^{-/-}$ hearts increased by 2-fold over WT ($P < 0.01$) and M-CK$^{-/-}$ hearts. Guanine nucleotide $\beta$-phosphoryl turnover (Fig. 3*B*) was 3-fold lower compared to $\beta$-phosphoryl turnover in adenine nucleotides (Fig. 1*B*), suggesting that NMPK-catalysed metabolic flux is lower than flux catalysed by AK.

Changes in glycolytic phosphotransfer were assessed by monitoring the appearance of $^{18}$O-labelled phosphoryls in G-6-P as a result of a reaction catalysed by hexokinase, the entry point into glycolysis (Fig. 3*C*). In WT hearts $^{18}$O labelling of G-6-P at 40 s was 8.1 ± 0.5% ($n = 3$), which was more than 10% of $\gamma$-ATP turnover (Fig. 1*C*). Deletion of M-CK resulted in an increase of G-6-P $^{18}$O labelling to 13.3 ± 0.8% ($P < 0.05$, $n = 3$). G-6-P $^{18}$O labelling was further increased to 26.8 ± 1.3% ($P < 0.01$, $n = 3$) in M-CK/ScCKmit$^{-/-}$ hearts, which corresponded to 37% of $\gamma$-ATP turnover. Thus, metabolic flux through the glycolytic phosphotransfer network is accelerated in single and especially double CK knockout hearts and may represent an important compensation alleviating myocardial energetic disturbances.

## Substrate uptake and utilization systems

To further define compensatory changes in glucose metabolism in CK-deficient hearts, we measured glucose uptake capacity in isolated perfused hearts by $^{31}$P NMR using the glucose analogue 2-deoxyglucose (2-DG) (Hopkins *et al.* 2004). The rate of 2-DG uptake (Fig. 4*A* and *B*) tended to be higher in the M-CK$^{-/-}$ hearts, 0.296 ± 0.02 mM min$^{-1}$, compared to the wild type and M-CK/ScCKmit$^{-/-}$ hearts, 0.234 ± 0.032 and 0.252 ± 0.025 mM min$^{-1}$, respectively. M-CK$^{-/-}$ and M-CK/ScCKmit$^{-/-}$ hearts displayed different insulin-stimulated 2-DG uptake kinetics, showing a trend towards elevated glucose transport capacity in both CK-deficient hearts (Fig. 4*C* and *D*). The rate of insulin-stimulated 2-DG uptake (Fig. 4*D*) was 2.16 ± 0.22, 3.03 ± 0.37 and 3.30 ± 0.41 mM min$^{-1}$ ($n = 5$ each, NS) in wild type, M-CK$^{-/-}$ and M-CK/ScCKmit$^{-/-}$ hearts, respectively.

Fuel selection plays an important role in cardiac metabolism. To assess the relative contribution of oxidizable substrates to acetyl-CoA production, which enters the Krebs cycle, hearts were perfused with $^{13}$C-enriched [U-$^{13}$C] glucose, [U-$^{13}$C] fatty acid, [2,4-$^{13}$C] $\beta$-hydroxybutyrate and [3-$^{13}$C] lactate. The contribution of each labelled substrate to oxidative metabolism was determined from $^{13}$C NMR spectra using the $^{13}$C isotopomer peak areas of the C3 and C4 of glutamate and modelling the tricarboxylic acid cycle fluxes (Malloy *et al.* 1990). Glucose utilization in wild type, M-CK$^{-/-}$ and M-CK/ScCKmit$^{-/-}$ hearts was 0.025 ± 0.007, 0.082 ± 0.02 ($P < 0.001$) and 0.032 ± 0.01 units (Fig. 4*E* and *F*), while lactate utilization was 0.248 ± 0.017, 0.308 ± 0.024 and 0.278 ± 0.008 units, respectively. Fatty acid utilization in wild type, M-CK$^{-/-}$ and M-CK/ScCKmit$^{-/-}$ hearts was 0.089 ± 0.007, 0.133 ± 0.009 and 0.122 ± 0.009 units, while ketone utilization was 0.187 ± 0.014, 0.164 ± 0.041 and 0.204 ± 0.049 units, respectively. Thus, M-CK$^{-/-}$ hearts have 2-fold higher glucose utilization compared to wild type hearts (Fig. 4*E*). In contrast, the overall substrate utilization profile for M-CK/ScCKmit$^{-/-}$ hearts was similar to wild type hearts, indicating either enhanced adaptation by other pathways or a limited ability to adjust substrate oxidation at the face of double genetic deficiency.

## Glycolytic and mitochondrial capacities and glucose tolerance

To assess changes in total glycolytic and mitochondrial capacities in M-CK/ScCKmit$^{-/-}$ mice, we measured maximal glucose conversion to lactate rate and citrate synthase activity, respectively, in both heart and skeletal muscle homogenates (Phillips *et al.* 2010). M-CK/ScCKmit$^{-/-}$ hearts and skeletal muscles have higher glycolytic capacity compared to wild type (Fig. 5*A* and *B*). The maximal lactate production rate was 3.1 ± 0.1 and 4.3 ± 0.3 $\mu$mol (g wet wt)$^{-1}$ min$^{-1}$ ($n = 6$, $P < 0.01$) in wild type and M-CK/ScCKmit$^{-/-}$ hearts, respectively. In wild type and M-CK/ScCKmit$^{-/-}$ skeletal muscles, the lactate production rate was 14.1 ± 0.1 and 17.6 ± 0.3 $\mu$mol (g wet wt)$^{-1}$ min$^{-1}$ ($n = 6$, $P < 0.001$), respectively. Heart and especially skeletal muscle of

M-CK/ScCKmit$^{-/-}$ mice had higher citrate synthase activity indicating enhanced mitochondrial capacity (Fig. 5*C*). Citrate synthase activities were $27.1 \pm 0.4$ and $31.4 \pm 1.4$ $\mu$mol (g wet wt)$^{-1}$ min$^{-1}$ ($n = 6$, $P < 0.05$) in hearts and $15.2 \pm 0.6$ and $30.7 \pm 2.1$ $\mu$mol (g wet wt)$^{-1}$ min$^{-1}$ ($n = 6$, $P < 0.001$) in skeletal muscles of wild type and M-CK/ScCKmit$^{-/-}$ mice, respectively. In accord with these findings M-CK/ScCKmit$^{-/-}$ mice had a better glucose tolerance (IPGTT) (Fig. 5*D*), indicating a higher glucose metabolizing capacity after glucose load. A separate simultaneous analysis of glucose tolerance (OGTT), insulin levels and insulin tolerance (ITT) (Supplemental Fig. S1*A*, *B* and *C*) revealed that CK deficiency is associated with increased glucose-induced insulin response and better insulin tolerance which could contribute to improved glucose homeostasis. As presented in Fig. S1*D*, an apparent compensatory increase in the CK-B isoform (Fig. S1*D*), which is the major CK isoform remaining in transgenic muscle, would also facilitate energetic compensation.

## Evaluation of the dynamic metabolomic phenotype

Principal component analysis (PCA) and partial least-squares discriminant analysis (PLS-DA) pattern recognition techniques allowed clustering of all metabolic and flux analysis data and discrimination among groups (Fig. 6 and Supplemental Fig. S2). The PLS-DA score plot (Fig. 6*A*) shows clear separation among groups based on metabolite levels and turnover/$^{18}$O-labelling rates indicating unique dynamic metabolic profiles for

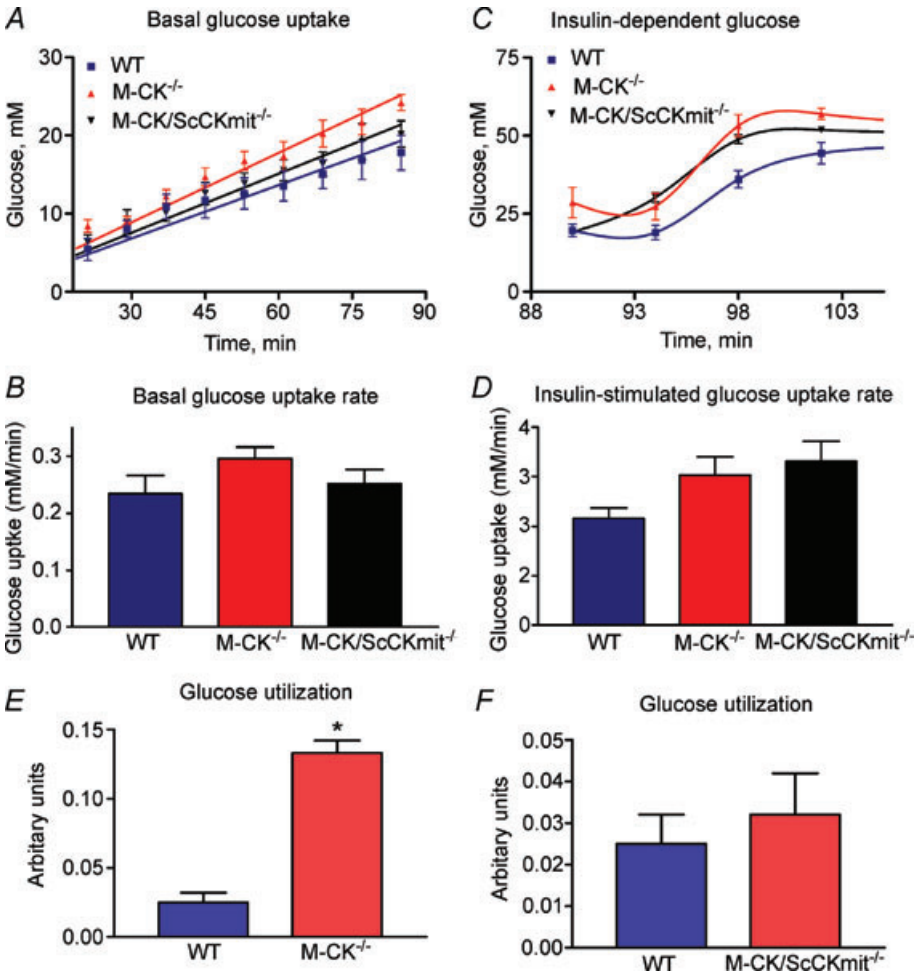


**Figure 4. Adjustments in glucose uptake and substrate utilization in CK-deficient hearts**
*A* and *B*, basal glucose (2-DG) uptake in wild type (WT), M-CK$^{-/-}$ and M-CK/ScCKmit$^{-/-}$ hearts. *C* and *D*, insulin-stimulated glucose (2-DG) uptake in WT, M-CK$^{-/-}$ and M-CK/ScCKmit$^{-/-}$ hearts. The insulin-stimulated glucose uptake rates have been calculated for each individual heart for the 15 min infusion of insulin (i.e. in the time from 90 to 105 min). The averaged data for each group are presented. *E* and *F*, glucose utilization in WT, M-CK$^{-/-}$ and M-CK/ScCKmit$^{-/-}$ hearts ($n = 5$ each). *$P < 0.05$.

wild type, M-CK$^{-/-}$ and M-CK/ScCKmit$^{-/-}$ hearts. The values of $R^2 = 0.61$ and $Q^2 = 0.79$ indicate the validity of the method and that the model was stable and good to fitness and prediction (Fig. S 2). The VIP values, a weighted sum of squares of the PLS weight which indicates the importance of the variable to the whole model, were calculated to identify the most important molecular variables for the clustering of all three groups (Fig. 6*A*, right panel). The results show the importance of parameters of glycolytic metabolism (lactate uptake, G-6-P $^{18}$O labelling and glucose uptake/utilization), AK phosphotransfer ($\beta$-ATP/$\beta$-ADP $^{18}$O labelling, AK flux), $P_i$/ATPase rate (Pi $^{18}$O labelling and compartmentation) and adenine (ATP turnover, $\gamma$-ATP $^{18}$O labelling, ATP/ADP ratio and ATP, ADP and AMP levels) and guanine (GTP $\gamma/\beta$-phosphoryl turnover) nucleotide metabolism in group classification.

A separate pair-wise PLS-DA analysis of wild type and M-CK$^{-/-}$ ($R^2 = 0.57$, $Q^2 = 0.91$) and wild type and M-CK/ScCKmit$^{-/-}$ ($R^2 = 0.69$, $Q^2 = 0.91$) hearts (Fig. 6*B* and *C*) allowed side-by-side comparison of metabolic variables important in phenotype determination and group separation. The right panels represent regression coefficient plots of metabolic variables in the PLS-DA model; larger coefficient values (positive or negative) indicate a stronger correlation with group metabolic profile classification. To extract the most important variables, variable importance in projection (VIP) statistics and loading weights were utilized (Fig. S2). Loading plots indicate those metabolites responsible for the clustering of groups (Fig. S2*B*). This analysis revealed that the metabolomic phenotype of M-CK$^{-/-}$ hearts (Fig. 6*B*, right panel) is characterized by the higher glucose uptake and utilization, lactate uptake and G-6-P turnover rates while the metabolomic profile of M-CK/ScCKmit$^{-/-}$ hearts (Fig. 6*C*, right panel) is characterized by a higher G-6-P turnover rate, G-6-P level, glycolytic capacity, $\gamma/\beta$-phosphoryl of GTP turnover as well as $\beta$-ATP and $\beta$-ADP turnover and AK flux.

## Discussion

Using new experimental and systems biology approaches, the organization and arrangement of cellular energetic relays into a robust network and the significance of metabolic dynamics in sustaining energy homeostasis and signal transduction can now be investigated (Dzeja *et al.* 1998, 2007*a*; Bose *et al.* 2003; Saks *et al.* 2006; Chung *et al.* 2010; Ingwall & Shen, 2010). CK represents the most active phosphotransfer enzyme in excitable tissues and plays a central role in high-energy phosphoryl transfer and in the distribution network, maintaining a stable

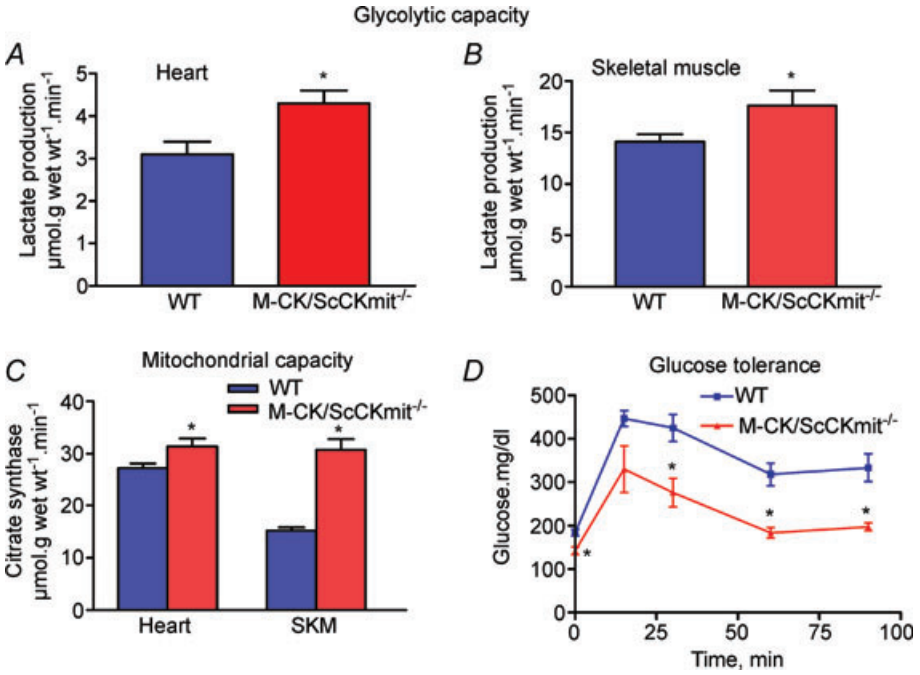


**Figure 5. Increased muscle glycolytic and mitochondrial capacities and glucose tolerance in CK-deficient mice**
*A* and *B*, glycolytic capacities in heart and skeletal muscles measured as maximal glucose conversion to lactate rate; *C*, mitochondrial capacities in heart and skeletal muscles assessed by citrate synthase activity; *D*, intraperitoneal glucose tolerance test (IPGTT) in WT and M-CK/ScCKmit$^{-/-}$ mice. *$P < 0.05$, $n = 5$ in each group.

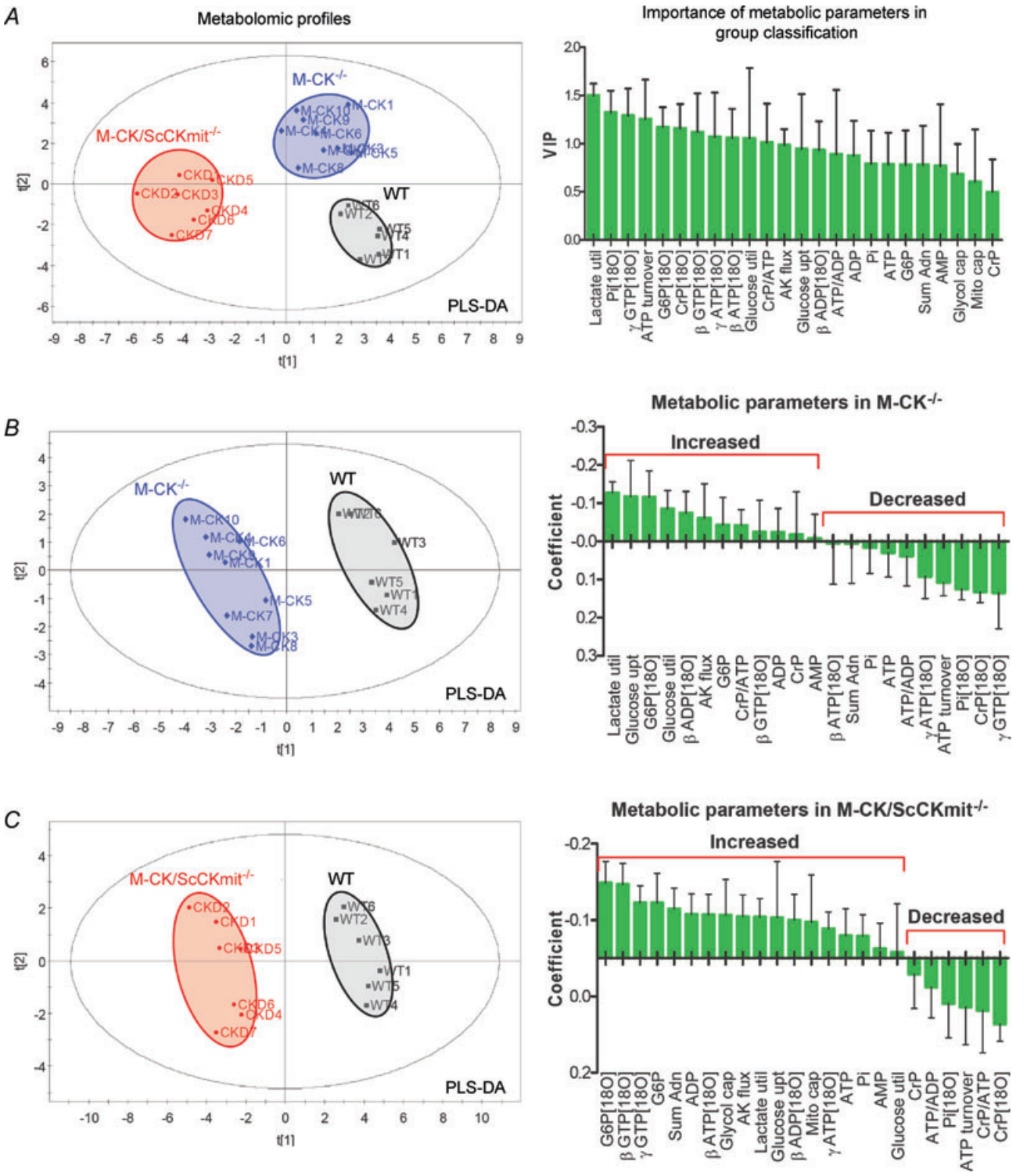


**Figure 6. Metabolomic profiles of WT, M-CK$^{-/-}$ and M-CK/ScCKmit$^{-/-}$ hearts**
*A* (left panel), PLS-DA score plot shows clear separation among groups based on metabolite levels and turnover/$^{18}$O-labelling rates indicating different metabolic profiles of WT, M-CK$^{-/-}$ and M-CK/ScCKmit$^{-/-}$ hearts ($R^2 = 0.87$, $Q^2 = 0.82$); right panel represents plot of variable importance in the projection (VIP) signifying importance of metabolites in discriminating between metabolomic profiles of the groups in the PLS-DA model. *B* and *C* (left panels), PLS-DA analysis of WT *vs*. M-CK$^{-/-}$ ($R^2 = 0.95$, $Q^2 = 0.88$) and WT *vs*. M-CK/ScCKmit$^{-/-}$ ($R^2 = 0.97$, $Q^2 = 0.92$) hearts separately; right panels represent regression coefficient plots of metabolic variables in the PLS discriminating model; larger coefficient values (positive or negative) indicate a stronger correlation with group metabolic profile classification, $n = 4$–6 in each group.

and efficient cellular bioenergetic infrastructure. Loss of CK activity and creatine content are hallmarks of cardiovascular disease (Ingwall *et al.* 1985; Ingwall, 2009; Ingwall & Shen, 2010). Here, a wide range of metabolic and flux interrogations of mouse hearts genetically manipulated to lack either the gene for M-CK or for both M-CK and ScCKmit have been used to define rearrangements in the cellular bioenergetic infrastructure, unveiling compensatory mechanisms elicited by chronic decreases in one or both of the major CK isozymes in the heart. Each type of CK-deficient heart has a unique signature of energy metabolism dynamics, substrate utilization and metabolomic profiles indicating rewiring in CK, AK, guanine nucleotide and glycolytic enzyme-catalysed phosphotransfer circuits and adjustments in the entire cellular energetic system. Induced compensatory phosphotransfer and mitochondria/glycolytic capacity mechanisms combine to maintain near-normal energy homeostasis in CK-deficient hearts. This new information indicates the significance of integrated CK-, AK-, guanine nucleotide- and glycolytic enzyme-catalysed phosphotransfer networks in supporting robustness of energy supply and providing mechanisms for energetic plasticity critical in compensating for cellular energetic deficits.

The contribution of CK-catalysed reactions to phosphoryl transfer in the heart depends on the total catalytic capacity, intracellular localization of CK isoforms and the ability of sequential CK catalysis to propagate displacement of the ATP/ADP equilibrium throughout cellular compartments (Ingwall, 1991; Wallimann *et al.* 1992; van Deursen *et al.* 1993; Dzeja *et al.* 1998; Saks *et al.* 2006, 2007; Wyss *et al.* 2007). A high rate of unidirectional phosphoryl exchange in phosphotransfer relay systems is necessary to promote metabolic flux wave propagation and high-energy phosphoryl transfer by ligand conduction mechanism (Dzeja *et al.* 1998; Dzeja & Terzic, 2003, 2007). $^{18}$O labelling analysis in hearts deficient in the major CK isoforms indicates that net phosphoryl transfer between ATP generation and utilization sites is coupled to a smaller number of phosphoryl exchange events in phosphotransfer networks, which could limit the efficiency of energy transfer. This interpretation is supported by the diminished $P_i/\gamma$-ATP $^{18}$O-labelling ratio, an indicator of energetic communication, observed here in CK-deficient hearts and by the inability to maintain normal global ATP/ADP ratios and high free energy of ATP hydrolysis ($\Delta G_{ATP}$) under high work load (Saupe *et al.* 1998, 2000).

CK activity of M-CK$^{-/-}$ and M-CK/ScCKmit$^{-/-}$ hearts was incrementally reduced leading to decreases in CK flux as assessed by the rate of appearance of $^{18}$O-labelled phosphoryls in PCr. Yet overall, ATP synthesis rate measured as oxygen consumption (Saupe *et al.* 1998) and, as reported here, as the rate of appearance of $^{18}$O-labelled phosphoryls in $\gamma$-ATP, did not differ among wild type, M-CK or M-CK/ScCKmit$^{-/-}$ hearts. Estimates of isovolumic contractile performance were also unchanged, although there was a trend for lower RPP for M-CK/ScCKmit$^{-/-}$ hearts (by ∼20%). Total creatine content was also unchanged (Saupe *et al.* 1998). The smaller pool size of metabolically active $P_i$ and the decreased $P_i/\gamma$-ATP $^{18}$O-labelling ratio, together with a trend to increased $\gamma$-ATP $^{18}$O labelling observed for both CK-deficient hearts indicate less efficient phosphotransfer energetics. Nonetheless, these observations suggest that the substantial decreases in CK flux in M-CK$^{-/-}$ and M-CK/ScCKmit$^{-/-}$ hearts are well compensated.

Our data support previous studies indicating that the cardiac muscle is characterized by remarkable stability of intracellular PCr and ATP contents during workload and respiration rate changes (Balaban *et al.* 1986), suggesting that efficient communication systems operate between ATP consumption and ATP synthesis sites (Dzeja & Terzic, 2003). Moreover, in the *in vivo* normal heart redundant multiple supporting systems of myocardial ATP production, transport and utilization exist, such that inhibition of one mechanism does not impair the normal left ventricular contractile performance (Dzeja *et al.* 2000; Dzeja & Terzic, 2003; Xiong *et al.* 2011). The decrease in total CK activity does not cause significant changes in cardiac contractility and heart energetics under basal conditions; however, the CK system is critically necessary to maintain optimal heart energy cycle and function at increased workloads (Saupe *et al.* 1998; Spindler *et al.* 2004). Other studies have found that the myocardium in CK-deficient mice is characterized by reduced perfusion and reduced maximal contraction velocity, suggesting that the myocardial hypertrophy seen in these mice cannot fully compensate for the absence of the CK system (Nahrendorf *et al.* 2006). Mice deficient in creatine synthesis, when acutely stressed by inotropic stimulation or ischaemia/reperfusion, exhibit a markedly abnormal phenotype, demonstrating that an intact, high-capacity CK/PCr system is required for situations of increased cardiac work or acute stress (ten Hove *et al.* 2005). Reduced CK flux is the most prominent energetic abnormality in human heart failure and myocardial infarction (Bottomley *et al.* 2009). In experimental heart failure diminished CK activity correlates with lower ATP levels and longer duration of atrial fibrillation, and decline in CK activity can be prevented by the vasopeptidase inhibitor omapatrilat and reversed in recovery from heart dysfunction (Shen *et al.* 2005; Cha *et al.* 2006). In a similar study it was concluded that a severely altered myocardial CK system could contribute to left ventricle dysfunction in congestive heart failure hearts (Ye *et al.* 2001).

The candidate compensatory phosphotransfer pathways include other CK isozymes, AK, and

guanine nucleotide and glycolytic enzyme-catalysed systems. Deletion of the gene for M-CK alone did not elicit significant changes in AK, GTP or NMPK phosphotransfer rates. However, glucose transport rate, phosphorylation by hexokinase and oxidation all increased. The functional load on the remaining CK isozymes (BB-CK and ScCKmit) increased and partially compensated for the loss of MM-CK activity. In contrast, deletion of both M-CK and ScCKmit genes led to substantial remodelling of all phosphotransfer pathways. Flux through the remaining BB-CK increased. Phosphotransfer flux through the AK system increased by 85%, GTP phosphoryl exchange rose by ∼25%, NMPK-catalysed $\beta$-GTP phosphoryl flux doubled and markers of glycolytic phosphotransfer and ATP production increased, including insulin-stimulated glucose uptake and formation of G-6-P by hexokinase. This was accompanied by increases in total heart and skeletal muscle glycolytic capacity and glucose tolerance. Despite increases in AK metabolic flux in M-CK/ScCKmit$^{-/-}$ hearts, combined CK and AK phosphotransfer capacity was 50% lower, suggesting that other phosphotransfer pathways provide an unexpectedly large energetic compensation (Dzeja *et al.* 1998, 2004; de Groof *et al.* 2001; Ventura-Clapier *et al.* 2004). Absence of ScCKmit in the mitochondrial intermembrane can be compensated by AK2 phosphotransfer, which is an integral part of the cellular energetic infrastructure and is critical for ATP export (Dzeja & Terzic, 2003) (Fig. 7). The significance of the circuit arrangement of mitochondrial and cellular energetic systems is highlighted by recent findings that deletion of the AK2 gene is embryonically lethal in *Drosophila* and mice due to severe disturbances in mitochondrial structure and energetics (Fujisawa *et al.* 2009; Zhang *et al.* 2010). Below we discuss these different compensatory energetic systems (Fig. 7) and rearrangements in metabolomic phenotypes.

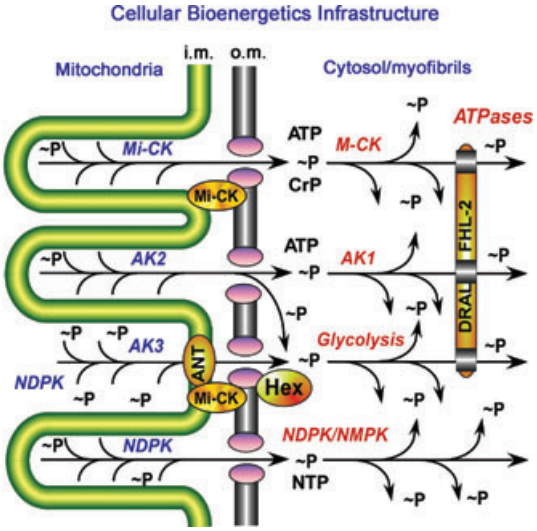


**Figure 7. Integrated model of cellular phosphotransfer circuits facilitating high-energy phosphoryl (~P) export from mitochondria and distribution to remote cellular ATPases**
Intramitochondrial, intermembrane and cytosolic phosphotransfer enzymes (CK, AK, glycolytic and NDPK/NMPK) facilitate nucleotide exchange between mitochondria and ATP consumption sites. Deletion of Mi-CK or AK2 compromises nucleotide exchange and AK2 null mutation is embryonically lethal (Spindler *et al.* 2002; Fujisawa *et al.* 2009; Zhang *et al.* 2010) while presence of NDPK is necessary for processing of nucleoside diphosphates (Lacombe *et al.* 2009). In myofibrils, phosphotransfer enzymes are positioned close to ATP utilization sites by interaction with scaffold protein DRAL/FHL-2 (down-regulated in rhabdomyosarcoma LIM domain protein/four-and-a-half LIM domain protein)attached to titin (Lange *et al.* 2002; Dzeja *et al.* 2007*a*). Reduction of DRAL/FHL-2 level is associated with disruption of the normal subcellular localization of metabolic enzymes in human heart failure (Bovill *et al.* 2009). Abbreviations: Mi-CK and M-CK, mitochondrial and cytosolic isoforms of CK, respectively; AK1 and AK2, cytosolic and mitochondrial isoforms of AK, respectively; AK3, mitochondrial matrix AK isoform; ANT, adenine nucleotide translocator; Hex, hexokinase; NDPK/NMPK, nucleoside di- and mono-phosphate kinases; DRAL/FHL-2, phosphotransfer enzyme anchor LIM domain protein; i.m. and o.m., inner and outer membranes, respectively.

In mammalian cells guanine nucleotides provide energetic support for synthetic, signal transduction and nuclear transport processes (Dzeja *et al.* 2002; Dzeja & Terzic, 2003; Hippe *et al.* 2009). Here, turnover of $\gamma$- and $\beta$-phosphoryls of GTP, reflecting metabolic flux through NDPK, the Krebs cycle enzyme succinyl CoA synthase and NMPK, was augmented only with the severe CK deficiency in M-CK/ScCKmit$^{-/-}$ hearts. The CK reaction can phosphorylate guanine nucleotides and regulate GTP-dependent protein synthesis and signal transduction processes (Wallimann *et al.* 1992). Results presented here suggest that lack of CK-catalysed guanine nucleotide phosphotransfer in M-CK/ScCKmit$^{-/-}$ hearts is partially compensated by the upregulation of the intrinsic guanylate metabolism (Zeleznikar *et al.* 1990).

In recent years, evidence has shown that the glycolytic pathway can function in energy transfer and distribution critical for energetic support of remote ATP-consuming processes (Fig. 7) (Dzeja *et al.* 1998, 2007*a*; Dzeja & Terzic, 2003). This function is accomplished through a network of glycolytic high-energy phosphoryl transfer enzymes extending from mitochondria to ATP utilization sites in myofibrils, nucleus and sarcolemma (Dzeja *et al.* 1998; de Groof *et al.* 2001; Dzeja & Terzic, 2003; Chung *et al.* 2010) (Fig. 7). G-6-P $^{18}$O-labelling analysis indicates that glycolytic phosphotransfer through the hexokinase step, an entry-point into glycolysis, is accelerated in both M-CK$^{-/-}$ and M-CK/ScCKmit$^{-/-}$ hearts and thus contributes to the compensation for CK deficits. The changes in $P_i$ $^{18}$O-labelling kinetics in CK-deficient hearts observed here indicate alterations in the feedback communication between heart work and mitochondrial respiration. Accelerated GAPDH–PGK and other glycolytic phosphotransfer reactions, facilitating

$P_i$ transfer, could explain the kinetic entrapment, i.e. decreased metabolic pool size and increased $P_i$ compartmentation/channeling in CK-deficient hearts (Bendahan *et al.* 1990; Dzeja *et al.* 2004).

Additional evidence supporting a contribution of increased glycolysis to compensate for CK deficits comes from measurement of glucose uptake and utilization rates and measures of glucose capacity. M-CK$^{-/-}$ hearts had a slight increase in basal glucose uptake rate, faster insulin-dependent glucose uptake reflecting faster GLUT 4 trafficking, faster $^{18}$O labelling of G-6-P, and slightly increased glycolytic enzyme capacity. M-CK/ScCKmit$^{-/-}$ hearts displayed faster kinetics of insulin-dependent glucose uptake, faster G-6-P $^{18}$O labelling, greater glycolytic and mitochondrial capacities and greater whole-body glucose tolerance. In addition, improved glucose tolerance in CK deficiency was associated with increased glucose-induced insulin response and sensitivity indicating robustness of metabolic signalling systems. Since energetic ($\Delta G_{ATP}$) and cardiac performance abnormalities were more pronounced in M-CK/ScCKmit$^{-/-}$ hearts, the smaller contribution of glucose utilization to ATP synthesis in M-CK/ScCKmit$^{-/-}$ hearts may indicate limited utility and compensatory potential of glycolysis in severe conditions of CK deficits as can occur in heart failure (Saupe *et al.* 1998, 2000).

These results are consistent with studies of CK-deficient muscles by others. CK-deficient skeletal muscle exhibits accelerated glycogenolysis during contraction (Katz *et al.* 2003). Increased activities of glycolytic enzymes such as pyruvate kinase and GAPDH were found in hearts of CK knockout animals (Ventura-Clapier *et al.* 1995; Aksentijevic *et al.* 2010). M-CK-deficient cardiomyocytes display a higher sensitivity to glycolytic inhibition manifested in premature opening of ATP-sensitive potassium channels and shortening of action potential as compared to wild type (Abraham *et al.* 2002), suggesting a greater reliance on glycolytic metabolism. Taken together, these results suggest that activation of high-energy phosphoryl transfer through the glycolytic pathway is an important adaptive mechanism in both cardiac and skeletal muscle with compromised CK catalysis.

Current progress in metabolic research is highlighted by identification of molecular players and their interactions, and by applying system and network approaches to cell metabolism including proteomic and metabolomic profiling (Saks *et al.* 2007; Feala *et al.* 2008; Ashrafian & Neubauer, 2009; Dzeja & Terzic, 2009; Agnetti *et al.* 2011). Here, using advanced metabolomic analyses, unique metabolic signatures for M-CK$^{-/-}$ and M-CK/ScCKmit$^{-/-}$ hearts and rearrangements in metabolic networks were revealed by PLS-DA pattern recognition technique allowing clustering of all metabolic data and discrimination between groups (Le Moyec *et al.* 2005; Rayens & Andersen, 2006). PLS-DA analysis demonstrates good separation of wild type, M-CK$^{-/-}$ and M-CK/ScCKmit$^{-/-}$ hearts based on metabolite levels and their turnover/$^{18}$O-labelling rates and substrate metabolism. The analysis demonstrates the importance of parameters of glycolytic metabolism, adenylate kinase phosphotransfer, $P_i$ metabolism and nucleotide metabolism in group classification. The metabolomic phenotype of M-CK$^{-/-}$ hearts is characterized primarily by higher glucose utilization and G-6-P turnover rates while the metabolomic profile of M-CK/ScCKmit$^{-/-}$ hearts was distinguished by higher G-6-P turnover rate, G-6-P level and glycolytic capacity, $\gamma/\beta$-phosphoryl of GTP turnover as well as $\beta$-ATP/$\beta$-ADP turnover and AK flux. These metabolomic changes indicate a system-wide response of cell energy metabolism to deletion of one significant node in the network. The observed metabolic perturbations and network rearrangements in CK deficiency support the system bioenergetics concept that robustness and dynamics of phosphotransfer networks provide an intracellular energetic continuum coupling discrete mitochondrial energetic units with remote ATP utilization sites that facilitate high-energy phosphoryl exchange and energetic efficiency (Fig. 7) (Saks *et al.* 2006; Dzeja *et al.* 2007*a*; Ingwall & Shen, 2010).

## Conclusions and general implications

In summary, the extensive remodelling of intracellular energetic and substrate utilization networks that occurs in hearts due to chronic CK deficiency emphasizes the importance of the CK-catalysed circuit in facilitated high-energy phosphoryl (~P) flow and distribution, which are required for efficiency and robustness of the whole cellular energetic system (Fig. 7). Compensation provided by other CK isozymes, AK, guanine nucleotide and glycolytic phosphotransfer systems in CK-deficient muscles indicates their integral role in facilitating high-energy phosphoryl exchange between intramitochondrial compartments and ATP-utilising sites especially under conditions of genetic or metabolic stress. Such energetic re-wiring together with increased mitochondrial and glycolytic capacities defines an adaptive metabolomic phenotype of CK deficiency. However, there could be physiological conditions where protracted heart metabolic load associated with stress could lead to decreased myocardial creatine levels and CK metabolic flux which may not be well compensated by other pathways (Neubauer *et al.* 1997; Shen *et al.* 2005; Bottomley *et al.* 2009; Aksentijevic *et al.* 2010). Moreover, chronic metabolic stress or diabetic conditions could also exhaust compensatory mechanisms such as glycolysis contributing to heart failure (Kingsley *et al.* 1991). As was concluded earlier, a gradual accumulation of defects at various

steps in the myocardial energetic system, along with compromised compensatory mechanisms, precipitates failure of the whole cardiac energetic infrastructure, ultimately contributing to myocardial dysfunction (Dzeja *et al.* 2000). Systemic mechanisms uncovered here of adaptation to chronic CK deficiency open new avenues for development of treatment strategies of cardiovascular diseases aimed at protection and recovery of CK activity and creatine content and stimulation of the alternative phosphotransfer pathways. Increasing heart energetic reserve and unloading stress on the metabolic system through resynchronization, ventricular assist device or metabolic rejuvenation therapies would facilitate recovery and gradual repair of myocardial functional and energetic infrastructure (Cha *et al.* 2006; Malliaras *et al.* 2009; Ingwall & Shen, 2010; Obrzut *et al.* 2010). Thus, rearrangements in the dynamics of intracellular phosphotransfer and substrate metabolic networks defined here advance our understanding of the cellular energetic infrastructure and provide perspectives for targeted regulation of cellular energy homeostasis in stress and disease states.

## References


Abraham MR, Selivanov VA, Hodgson DM, Pucar D, Zingman LV, Wieringa B *et al.* (2002). Coupling of cell energetics with membrane metabolic sensing. Integrative signaling through creatine kinase phosphotransfer disrupted by M-CK gene knock-out. *J Biol Chem* **277**, 24427–24434.

Agnetti G, Husberg C & Van Eyk JE (2011). Divide and conquer: the application of organelle proteomics to heart failure. *Circ Res* **108**, 512–526.

Aksentijevic D, Lygate CA, Makinen K, Zervou S, Sebag-Montefiore L, Medway D *et al.* (2010). High-energy phosphotransfer in the failing mouse heart: role of adenylate kinase and glycolytic enzymes. *Eur J Heart Fail* **12**, 1282–1289.

Ashrafian H & Neubauer S (2009). Metabolomic profiling of cardiac substrate utilization: fanning the flames of systems biology? *Circulation* **119**, 1700–1702.

Balaban RS, Kantor HL, Katz LA & Briggs RW (1986). Relation between work and phosphate metabolite in the in vivo paced mammalian heart. *Science* **232**, 1121–1123.

Bendahan D, Confort-Gouny S, Kozak-Reiss G & Cozzone PJ (1990). Pi trapping in glycogenolytic pathway can explain transient Pi disappearance during recovery from muscular exercise. A $^{31}$P NMR study in the human. *FEBS Lett* **269**, 402–405.

Boehm E, Ventura-Clapier R, Mateo P, Lechene P & Veksler V (2000). Glycolysis supports calcium uptake by the sarcoplasmic reticulum in skinned ventricular fibres of mice deficient in mitochondrial and cytosolic creatine kinase. *J Mol Cell Cardiol* **32**, 891–902.

Bose S, French S, Evans FJ, Joubert F & Balaban RS (2003). Metabolic network control of oxidative phosphorylation: multiple roles of inorganic phosphate. *J Biol Chem* **278**, 39155–39165.

Bottomley PA, Wu KC, Gerstenblith G, Schulman SP, Steinberg A & Weiss RG (2009). Reduced myocardial creatine kinase flux in human myocardial infarction: an *in vivo* phosphorus magnetic resonance spectroscopy study. *Circulation* **119**, 1918–1924.

Bovill E, Westaby S, Crisp A, Jacobs S & Shaw T (2009). Reduction of four-and-a-half LIM-protein 2 expression occurs in human left ventricular failure and leads to altered localization and reduced activity of metabolic enzymes. *J Thorac Cardiovasc Surg* **137**, 853–861.

Bruton JD, Dahlstedt AJ, Abbate F & Westerblad H (2003). Mitochondrial function in intact skeletal muscle fibres of creatine kinase deficient mice. *J Physiol* **552**, 393–402.

Cha YM, Dzeja PP, Redfield MM, Shen WK & Terzic A (2006). Bioenergetic protection of failing atrial and ventricular myocardium by vasopeptidase inhibitor omapatrilat. *Am J Physiol Heart Circ Physiol* **290**, H1686–H1692.

Cha YM, Dzeja PP, Shen WK, Jahangir A, Hart CY, Terzic A & Redfield MM (2003). Failing atrial myocardium: energetic deficits accompany structural remodeling and electrical instability. *Am J Physiol Heart Circ Physiol* **284**, H1313–H1320.

Chung S, Arrell DK, Faustino RS, Terzic A & Dzeja PP (2010). Glycolytic network restructuring integral to the energetics of embryonic stem cell cardiac differentiation. *J Mol Cell Cardiol* **48**, 725–734.

Crozatier B, Badoual T, Boehm E, Ennezat PV, Guenoun T, Su J *et al.* (2002). Role of creatine kinase in cardiac excitation-contraction coupling: studies in creatine kinase-deficient mice. *FASEB J* **16**, 653–660.

Dahlstedt AJ, Katz A, Tavi P & Westerblad H (2003). Creatine kinase injection restores contractile function in creatine-kinase-deficient mouse skeletal muscle fibres. *J Physiol* **547**, 395–403.

Dawis SM, Walseth TF, Deeg MA, Heyman RA, Graeff RM & Goldberg ND (1989). Adenosine triphosphate utilization rates and metabolic pool sizes in intact cells measured by transfer of $^{18}$O from water. *Biophy J* **55**, 79–99.

de Groof AJ, Oerlemans FT, Jost CR & Wieringa B (2001). Changes in glycolytic network and mitochondrial design in creatine kinase-deficient muscles. *Muscle Nerve* **24**, 1188–1196.

Drummond GB (2009). Reporting ethical matters in *The Journal of Physiology*: standards and advice. *J Physiol* **587**, 713–719.

Dzeja P, Chung S & Terzic A (2007*a*). Integration of adenylate kinase, glycolytic and glycogenolytic circuits in cellular energetics. In *Molecular System Bioenergetics: Energy for Life*, ed. Saks V, pp. 265–301. Wiley-VCH, Weinheim, Germany.

Dzeja P & Terzic A (2009). Adenylate kinase and AMP signaling networks: metabolic monitoring, signal communication and body energy sensing. *Int J Mol Sci* **10**, 1729–1772.

Dzeja PP, Bast P, Pucar D, Wieringa B & Terzic A (2007*b*). Defective metabolic signaling in adenylate kinase AK1 gene knock-out hearts compromises post-ischemic coronary reflow. *J Biol Chem* **282**, 31366–31372.

Dzeja PP, Bortolon R, Perez-Terzic C, Holmuhamedov EL & Terzic A (2002). Energetic communication between mitochondria and nucleus directed by catalyzed phosphotransfer. *Proc Natl Acad Sci U S A* **99**, 10156–10161.

Dzeja PP, Redfield MM, Burnett JC & Terzic A (2000). Failing energetics in failing hearts. *Curr Cardiol Reps* **2**, 212–217.

Dzeja PP & Terzic A (2003). Phosphotransfer networks and cellular energetics. *J Exp Biol* **206**, 2039–2047.

Dzeja PP & Terzic A (2007). Mitochondria-nucleus energetic communication: role for phosphotransfer networks in processing cellular information. In *Brain Energetics: Integration of Molecular and Cellular Processes*, ed. Gibson G & Dienel G, pp. 641–666. Springer, New York.

Dzeja PP, Terzic A & Wieringa B (2004). Phosphotransfer dynamics in skeletal muscle from creatine kinase gene-deleted mice. *Mol Cell Biochem* **256–257**, 13–27.

Dzeja PP, Vitkevicius KT, Redfield MM, Burnett JC & Terzic A (1999). Adenylate kinase-catalyzed phosphotransfer in the myocardium : increased contribution in heart failure. *Circ Res* **84**, 1137–1143.

Dzeja PP, Zeleznikar RJ & Goldberg ND (1996). Suppression of creatine kinase-catalyzed phosphotransfer results in increased phosphoryl transfer by adenylate kinase in intact skeletal muscle. *J Biol Chem* **271**, 12847–12851.

Dzeja PP, Zeleznikar RJ & Goldberg ND (1998). Adenylate kinase: kinetic behavior in intact cells indicates it is integral to multiple cellular processes. *Mol Cell Biochem* **184**, 169–182.

Feala JD, Coquin L, Paternostro G & McCulloch AD (2008). Integrating metabolomics and phenomics with systems models of cardiac hypoxia. *Prog Biophys Mol Biol* **96**, 209–225.

Feala JD, Coquin L, Zhou D, Haddad GG, Paternostro G & McCulloch AD (2009). Metabolism as means for hypoxia adaptation: metabolic profiling and flux balance analysis. *BMC Syst Biol* **3**, 91.

Fujisawa K, Murakami R, Horiguchi T & Noma T (2009). Adenylate kinase isozyme 2 is essential for growth and development of Drosophila melanogaster. *Comp Biochem Physiol B Biochem Mol Biol* **153**, 29–38.

Gohil VM, Sheth SA, Nilsson R, Wojtovich AP, Lee JH, Perocchi F *et al.* (2010). Nutrient-sensitized screening for drugs that shift energy metabolism from mitochondrial respiration to glycolysis. *Nat Biotechnol* **28**, 249–255.

Hardie DG (2011). AMP-activated protein kinase: a cellular energy sensor with a key role in metabolic disorders and in cancer. *Biochem Soc Trans* **39**, 1–13.

Hippe HJ, Wolf NM, Abu-Taha I, Mehringer R, Just S, Lutz S*et al.* (2009). The interaction of nucleoside diphosphate kinase B with Gbg dimers controls heterotrimeric G protein function. *Proc Natl Acad Sci U S A* **106**, 16269–16274.

Hopkins JC, Radda GK, Veech RL & Clarke K (2004). Accumulation of 2-deoxy-D-glucose-6-phosphate as a measure of glucose uptake in the isolated perfused heart: a $^{31}$P NMR study. *Metab Eng* **6**, 36–43.

Ingwall JS (1991). Whole-organ enzymology of the creatine kinase system in heart. *Biochem Soc Trans* **19**, 1006–1010.

Ingwall JS (2004). Transgenesis and cardiac energetics: new insights into cardiac metabolism. *J Mol Cell Cardiol* **37**, 613–623.

Ingwall JS (2006). Energetics of the failing heart: new insights using genetic modification in the mouse. *Arch Mal Coeur Vaiss* **99**, 839–847.

Ingwall JS (2009). Energy metabolism in heart failure and remodelling. *Cardiovasc Res* **81**, 412–419.

Ingwall JS, Kramer MF, Fifer MA, Lorell BH, Shemin R, Grossman W & Allen PD (1985). The creatine kinase system in normal and diseased human myocardium. *N Engl J Med* **313**, 1050–1054.

Ingwall JS & Shen W (2010). On energy circuits in the failing myocardium. *Eur J Heart Fail* **12**, 1268–1270.

Janssen E, Dzeja PP, Oerlemans F, Simonetti AW, Heerschap A, de Haan A *et al.* (2000). Adenylate kinase 1 gene deletion disrupts muscle energetic economy despite metabolic rearrangement. *EMBO J* **19**, 6371–6381.

Janssen E, Terzic A, Wieringa B & Dzeja PP (2003). Impaired intracellular energetic communication in muscles from creatine kinase and adenylate kinase (M-CK/AK1) double knock-out mice. *J Biol Chem* **278**, 30441–30449.

Jeninga EH, Schoonjans K & Auwerx J (2010). Reversible acetylation of PGC-1: connecting energy sensors and effectors to guarantee metabolic flexibility. *Oncogene* **29**, 4617–4624.

Jones RG & Thompson CB (2009). Tumor suppressors and cell metabolism: a recipe for cancer growth. *Genes Dev* **23**, 537–548.

Karl DM & Bossard P (1985). Measurement of microbial nucleic acid synthesis and specific growth rate by $^{32}PO_4$ and [$^3$H]adenine: field comparison. *Appl Environ Microbiol* **50**, 706–709.

Katz A, Andersson DC, Yu J, Norman B, Sandstrom ME, Wieringa B & Westerblad H (2003). Contraction-mediated glycogenolysis in mouse skeletal muscle lacking creatine kinase: the role of phosphorylase b activation. *J Physiol* **553**, 523–531.

Kingsley PB, Sako EY, Yang MQ, Zimmer SD, Ugurbil K, Foker JE & From AH (1991). Ischemic contracture begins when anaerobic glycolysis stops: a $^{31}$P-NMR study of isolated rat hearts. *Am J Physiol Heart Circ Physiol* **261**, H469–H478.

Kolwicz SC Jr & Tian R (2009). Metabolic therapy at the crossroad: how to optimize myocardial substrate utilization? *Trends Cardiovasc Med* **19**, 201–207.

Kuiper JW, van Horssen R, Oerlemans F, Peters W, van Dommelen MM, te Lindert MM *et al.* (2009). Local ATP generation by brain-type creatine kinase (CK-B) facilitates cell motility. *PLoS ONE* **4**, e5030.

Lacombe ML, Tokarska-Schlattner M, Epand RF, Boissan M, Epand RM & Schlattner U (2009). Interaction of NDPK-D with cardiolipin-containing membranes: structural basis and implications for mitochondrial physiology. *Biochimie* **91**, 779–783.

Lagresle-Peyrou C, Six EM, Picard C, Rieux-Laucat F, Michel V, Ditadi A *et al.* (2009). Human adenylate kinase 2 deficiency causes a profound hematopoietic defect associated with sensorineural deafness. *Nat Genet* **41**, 106–111.

Lange S, Auerbach D, McLoughlin P, Perriard E, Schafer BW, Perriard JC & Ehler E (2002). Subcellular targeting of metabolic enzymes to titin in heart muscle may be mediated by DRAL/FHL-2. *J Cell Sci* **115**, 4925–4936.

Le Moyec L, Valensi P, Charniot JC, Hantz E & Albertini JP (2005). Serum $^{1}$H-nuclear magnetic spectroscopy followed by principal component analysis and hierarchical cluster analysis to demonstrate effects of statins on hyperlipidemic patients. *NMR Biomed* **18**, 421–429.

Luptak I, Yan J, Cui L, Jain M, Liao R & Tian R (2007). Long-term effects of increased glucose entry on mouse hearts during normal aging and ischemic stress. *Circulation* **116**, 901–909.

Malliaras KG, Terrovitis JV, Drakos SG & Nanas JN (2009). Reverse cardiac remodeling enabled by mechanical unloading of the left ventricle. *J Cardiovasc Transl Res* **2**, 114–125.

Malloy CR, Sherry AD & Jeffrey FM (1988). Evaluation of carbon flux and substrate selection through alternate pathways involving the citric acid cycle of the heart by $^{13}$C NMR spectroscopy. *J Biol Chem* **263**, 6964–6971.

Malloy CR, Sherry AD & Jeffrey FM (1990). Analysis of tricarboxylic acid cycle of the heart using $^{13}$C isotope isomers. *Am J Physiol Heart Circ Physiol* **259**, H987–H995.

Metallo CM, Walther JL & Stephanopoulos G (2009). Evaluation of $^{13}$C isotopic tracers for metabolic flux analysis in mammalian cells. *J Biotechnol* **144**, 167–174.

Nahrendorf M, Streif JU, Hiller KH, Hu K, Nordbeck P, Ritter O *et al.* (2006). Multimodal functional cardiac MRI in creatine kinase-deficient mice reveals subtle abnormalities in myocardial perfusion and mechanics. *Am J Physiol Heart Circ Physiol* **290**, H2516–H2521.

Neubauer S, Horn M, Cramer M, Harre K, Newell JB, Peters W *et al.* (1997). Myocardial phosphocreatine-to-ATP ratio is a predictor of mortality in patients with dilated cardiomyopathy. *Circulation* **96**, 2190–2196.

Nicolay K, van Dorsten FA, Reese T, Kruiskamp MJ, Gellerich JF & van Echteld CJ (1998). In situ measurements of creatine kinase flux by NMR. The lessons from bioengineered mice. *Mol Cell Biochem* **184**, 195–208.

Noma T (2005). Dynamics of nucleotide metabolism as a supporter of life phenomena. *J Med Invest* **52**, 127–136.

Obrzut S, Tiongson J, Jamshidi N, Phan HM, Hoh C & Birgersdotter-Green U (2010). Assessment of metabolic phenotypes in patients with non-ischemic dilated cardiomyopathy undergoing cardiac resynchronization therapy. *J Cardiovasc Transl Res* **3**, 643–651.

Olson LK, Schroeder W, Robertson RP, Goldberg ND & Walseth TF (1996). Suppression of adenylate kinase catalyzed phosphotransfer precedes and is associated with glucose-induced insulin secretion in intact HIT-T15 cells. *J Biol Chem* **271**, 16544–16552.

Pannicke U, Honig M, Hess I, Friesen C, Holzmann K, Rump EM *et al.* (2009). Reticular dysgenesis (aleukocytosis) is caused by mutations in the gene encoding mitochondrial adenylate kinase 2. *Nat Genet* **41**, 101–105.

Phillips D, Ten Hove M, Schneider JE, Wu CO, Sebag-Montefiore L, Aponte AM *et al.* (2010). Mice over-expressing the myocardial creatine transporter develop progressive heart failure and show decreased glycolytic capacity. *J Mol Cell Cardiol* **48**, 582–590.

Pucar D, Bast P, Gumina RJ, Lim L, Drahl C, Juranic N *et al.* (2002). Adenylate kinase AK1 knockout heart: energetics and functional performance under ischemia-reperfusion. *Am J Physiol Heart Circ Physiol* **283**, H776–H782.

Pucar D, Dzeja PP, Bast P, Gumina RJ, Drahl C, Lim L *et al.* (2004). Mapping hypoxia-induced bioenergetic rearrangements and metabolic signaling by $^{18}$O-assisted $^{31}$P NMR and $^{1}$H NMR spectroscopy. *Mol Cell Biochem* **256–257**, 281–289.

Pucar D, Dzeja PP, Bast P, Juranic N, Macura S & Terzic A (2001). Cellular energetics in the preconditioned state: protective role for phosphotransfer reactions captured by $^{18}$O-assisted $^{31}$P NMR. *J Biol Chem* **276**, 44812–44819.

Pucar D, Janssen E, Dzeja PP, Juranic N, Macura S, Wieringa B & Terzic A (2000). Compromised energetics in the adenylate kinase AK1 gene knockout heart under metabolic stress. *J Biol Chem* **275**, 41424–41429.

Rayens WS & Andersen AH (2006). Multivariate analysis of fMRI data by oriented partial least squares. *Magn Reson Imaging* **24**, 953–958.

Rossi A (1975). $^{32}$P labelling of the nucleotides in alpha-position in the rabbit heart. *J Mol Cell Cardiol* **7**, 891–906.

Saks V, Dzeja P, Schlattner U, Vendelin M, Terzic A & Wallimann T (2006). Cardiac system bioenergetics: metabolic basis of the Frank-Starling law. *J Physiol* **571**, 253–273.

Saks V, Monge C, Anmann T & Dzeja P (2007). Integrated and organized cellular energetic systems: theories of cell energetics, compartmentation and metabolic channeling. In *Molecular System Bioenergetics: Energy for Life*, ed. Saks V, pp. 59–109. Wiley-VCH, Weinheim, Germany.

Saks VA, Khuchua ZA, Vasilyeva EV, Belikova O & Kuznetsov AV (1994). Metabolic compartmentation and substrate channelling in muscle cells. Role of coupled creatine kinases in *in vivo* regulation of cellular respiration–a synthesis. *Mol Cell Biochem* **133–134**, 155–192.

Saupe KW, Spindler M, Hopkins JC, Shen W & Ingwall JS (2000). Kinetic, thermodynamic, and developmental consequences of deleting creatine kinase isoenzymes from the heart. Reaction kinetics of the creatine kinase isoenzymes in the intact heart. *J Biol Chem* **275**, 19742–19746.

Saupe KW, Spindler M, Tian R & Ingwall JS (1998). Impaired cardiac energetics in mice lacking muscle-specific isoenzymes of creatine kinase. *Circ Res* **82**, 898–907.

Shen W, Spindler M, Higgins MA, Jin N, Gill RM, Bloem LJ *et al.* (2005). The fall in creatine levels and creatine kinase isozyme changes in the failing heart are reversible: complex post-transcriptional regulation of the components of the CK system. *J Mol Cell Cardiol* **39**, 537–544.

Spindler M, Meyer K, Stromer H, Leupold A, Boehm E, Wagner H & Neubauer S (2004). Creatine kinase-deficient hearts exhibit increased susceptibility to ischemia-reperfusion injury and impaired calcium homeostasis. *Am J Physiol Heart Circ Physiol* **287**, H1039–H1045.

Spindler M, Niebler R, Remkes H, Horn M, Lanz T & Neubauer S (2002). Mitochondrial creatine kinase is critically necessary for normal myocardial high-energy phosphate metabolism. *Am J Physiol Heart Circ Physiol* **283**, H680–H687.

Steeghs K, Benders A, Oerlemans F, de Haan A, Heerschap A, Ruitenbeek W *et al*. (1997). Altered $Ca^{2+}$ responses in muscles with combined mitochondrial and cytosolic creatine kinase deficiencies. *Cell* **89**, 93–103.

Taegtmeyer H, Goodwin GW, Doenst T & Frazier OH (1997). Substrate metabolism as a determinant for postischemic functional recovery of the heart. *Am J Cardiol* **80**, 3A–10A.

ten Hove M, Lygate CA, Fischer A, Schneider JE, Sang AE, Hulbert K *et al*. (2005). Reduced inotropic reserve and increased susceptibility to cardiac ischemia/reperfusion injury in phosphocreatine-deficient guanidinoacetate-N-methyltransferase-knockout mice. *Circulation* **111**, 2477–2485.

Tian R (2003). Transcriptional regulation of energy substrate metabolism in normal and hypertrophied heart. *Curr Hypertens Rep* **5**, 454–458.

Titman CM, Downs JA, Oliver SG, Carmichael PL, Scott AD & Griffin JL (2009). A metabolomic and multivariate statistical process to assess the effects of genotoxins in *Saccharomyces cerevisiae*. *Mol Biosyst* **5**, 1913–1924.

van Deursen J, Heerschap A, Oerlemans F, Ruitenbeek W, Jap P, ter Laak H & Wieringa B (1993). Skeletal muscles of mice deficient in muscle creatine kinase lack burst activity. *Cell* **74**, 621–631.

Ventura-Clapier R, Garnier A, Veksler V & Joubert F (2010). Bioenergetics of the failing heart. *Biochim Biophys Acta* **1813**, 1360–1372.

Ventura-Clapier R, Kaasik A & Veksler V (2004). Structural and functional adaptations of striated muscles to CK deficiency. *Mol Cell Biochem* **256–257**, 29–41.

Ventura-Clapier R, Kuznetsov AV, d'Albis A, van Deursen J, Wieringa B & Veksler VI (1995). Muscle creatine kinase-deficient mice. I. Alterations in myofibrillar function. *J Biol Chem* **270**, 19914–19920.

Wallimann T, Wyss M, Brdiczka D, Nicolay K & Eppenberger HM (1992). Intracellular compartmentation, structure and function of creatine kinase isoenzymes in tissues with high and fluctuating energy demands: the 'phosphocreatine circuit' for cellular energy homeostasis. *Biochem J* **281**, 21–40.

Wiechert W & de Graaf AA (1997). Bidirectional reaction steps in metabolic networks: I. Modeling and simulation of carbon isotope labeling experiments. *Biotechnol Bioeng* **55**, 101–117.

Wyss M, Braissant O, Pischel I, Salomons GS, Schulze A, Stockler S & Wallimann T (2007). Creatine and creatine kinase in health and disease – a bright future ahead? *Subcell Biochem* **46**, 309–334.

Xiong Q, Du F, Zhu X, Zhang P, Suntharalingam P, Ippolito J *et al*. (2011). ATP production rate via creatine kinase or ATP synthase *in vivo*: a novel superfast magnetization saturation transfer method. *Circ Res* **108**, 653–663.

Yang YC, Fann MJ, Chang WH, Tai LH, Jiang JH & Kao LS (2010). Regulation of sodium-calcium exchanger activity by creatine kinase under energy-compromised conditions. *J Biol Chem* **285**, 28275–28285.

Ye Y, Gong G, Ochiai K, Liu J & Zhang J (2001). High-energy phosphate metabolism and creatine kinase in failing hearts: a new porcine model. *Circulation* **103**, 1570–1576.

Zeleznikar RJ, Dzeja PP & Goldberg ND (1995). Adenylate kinase-catalyzed phosphoryl transfer couples ATP utilization with its generation by glycolysis in intact muscle. *J Biol Chem* **270**, 7311–7319.

Zeleznikar RJ & Goldberg ND (1991). Kinetics and compartmentation of energy metabolism in intact skeletal muscle determined from $^{18}O$ labeling of metabolite phosphoryls. *J Biol Chem* **266**, 15110–15119.

Zeleznikar RJ, Heyman RA, Graeff RM, Walseth TF, Dawis SM, Butz EA & Goldberg ND (1990). Evidence for compartmentalized adenylate kinase catalysis serving a high energy phosphoryl transfer function in rat skeletal muscle. *J Biol Chem* **265**, 300–311.

Zhang S, Nemutlu E & Dzeja P (2010). Metabolomic profiling of adenylate kinase $AK1^{-/-}$ and $AK2^{+/-}$ transgenic mice: effect of physical stress. *Circulation* **122**, A20435.

Zilversmit DB, Entenman C & Fishler MC (1943). On the calculation of "turnover time" and "turnover rate" from experiments involving the use of labeling agents. *J Gen Physiol* **26**, 325–331.

## Author contributions

All experiments were performed at the Division of Cardiovascular Medicine, Department of Medicine, Brigham and Women's Hospital and Harvard Medical School, Boston, MA, USA, Department of Biochemistry, University of Minnesota, MN, USA, and Division of Cardiovascular Diseases, Departments of Internal Medicine and Molecular Pharmacology and Experimental Therapeutics, Mayo Clinic, Rochester, MN, USA. P.P.D. and J.S.I. were involved in the conception and design of the studies. All authors were involved in the collection, analysis and interpretation of the data. P.P.D. was mainly responsible for drafting the article and critical input was obtained from all other authors. All authors were involved in drafting and/or revising the manuscript, and all approved the final version.

## Acknowledgements

This study is dedicated to the memory of the late Professor Nelson Goldberg, Department of Biochemistry, University of Minnesota, who initiated this study and contributed so much to our understanding of metabolic and signal transduction dynamics in the regulation of multiple cellular processes. This work was supported by the American Heart Association, Marriott Foundation and National Institutes of Health.